



T.C.
SELÇUK ÜNİVERSİTESİ
FEN BİLİMLERİ ENSTİTÜSÜ



**DETECTION OF BROKEN ROTOR BARS IN
INDUCTION MOTORS USING MOTOR
CURRENT SIGNATURE ANALYSIS (MCSA)**

Mohamed Ali MOHAMED

MASTER'S DEGREE THESIS

Mechatronics Engineering Department

September-2019
KONYA
All Rights Reserved

TEZ KABUL VE ONAYI

Mohamed Ali MOHAMED tarafından hazırlanan “Akim Spektrumu Analizini Kullanarak Asenkron Motor Rotor Çubuğu Hatalarının Tespiti” adlı tez çalışması 19/09/2019 tarihinde aşağıdaki jüri tarafından oy birliği ile Selçuk Üniversitesi Fen Bilimleri Enstitüsü Mekatronik Mühendisliği Anabilim Dalı’nda YÜKSEK LİSANS TEZİ olarak kabul edilmiştir.

Jüri Üyeleri

Başkan

Dr. Öğr. Üyesi Hulusi KARACA

Danışman

Doç. Dr. Hayri ARABACI

Üye

Dr. Öğr. Üyesi Mümtaz MUTLUER

İmza



Yukarıdaki sonucu onaylarım.

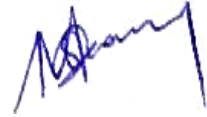
Prof. Dr. Mustafa YILMAZ
FBE Müdürü

TEZ BİLDİRİMİ

Bu tezdeki bütün bilgilerin etik davranış ve akademik kurallar çerçevesinde elde edildiğini ve tez yazım kurallarına uygun olarak hazırlanan bu çalışmada bana ait olmayan her türlü ifade ve bilginin kaynağına eksiksiz atıf yapıldığını bildiririm.

DECLARATION PAGE

I hereby declare that all information in this document has been obtained and presented in accordance with academic rules and ethical conduct. I also declare that, as required by these rules and conduct, I have fully cited and referenced all material and results that are not original to this work.



Signature

Mohamed Ali MOHAMED

Date: 19/09/2019

ÖZET

YÜKSEK LİSANS TEZİ

AKIM SPEKTRUMU ANALİZİNİ KULLANARAK ASENKRON MOTOR ROTOR ÇUBUĞU HATALARININ TESPİTİ

Mohamed Ali MOHAMED

**Selçuk Üniversitesi Fen Bilimleri Enstitüsü
Mekatronik Mühendisliği Anabilim Dalı**

Danışman: Doç. Dr. Hayri ARABACI

2019, 59 Sayfa

Jüri

Asenkron motorlar, basit yapıları, ucuz olmaları ve güvenilirlikleri nedeniyle elektro-mekanik enerji dönüşümünde yaygın olarak kullanılan makinelerdir. Sağlamlığına rağmen nadiren de olsa arızalanabilmektedirler. Asenkron motorların yaygın kullanımı dolayısıyla bağlı olduğu işlemlerin önemi sebebiyle bu alanda çok sayıda çalışma yapılmış ve hala arıza teşhisi üzerine çalışmalar devam etmektedir.

Bu çalışmada kırık rotor çubuğu hatalarının bir makine öğrenme yaklaşımı ile tespiti sunulmuştur. Bu yaklaşımda hataların tespiti için motorun bir fazından alınan akım kullanıldı. Akım verileri Hall etkili akım sensörü ile alındı ve kaydedildi. Sinyaller çevrim dışı olarak işlendi ve yüksek frekanslı bileşenler çıkarıldı. Frekans alanına inceleme için FFT algoritması uygulandı. Temel bileşen analizi kullanılarak özellik çıkarımı ve veri azaltma yapıldı. Her bir arıza ve sağlam durumu için nominal yük altında alınmış 24 örnek kullanıldı.

Çalışmada iki sınıflandırma yaklaşımı önerildi. Yaklaşım 1; tek aşamada sınıflandırma gerçekleştirir. Yaklaşım 2; iki adımda sınıflandırma gerçekleştirir. Geliştirilen yaklaşımları değerlendirmek için çeşitli testler yapıldı. Algoritmaların değerlendirilmesinde; genel sınıflandırma doğruluğu, yanlış pozitif ve yanlış negatif oranlar anahtar faktörler olarak kullanıldı. Önerilen yaklaşım sayesinde rotor arızaları %4,2 lik hata ile sınıflandırıldı ve hatalı rotor %100 doğrulukla teşhis edildi.

Anahtar Kelimeler: asenkron motor, sincap kafesi, destek vektör makineleri, temel bileşen analizi, arıza teşhisi, kırık rotor çubuğu.

ABSTRACT

MS THESIS

**DETECTION OF BROKEN ROTOR BARS IN INDUCTION MOTORS USING
MOTOR CURRENT SIGNATURE ANALYSIS (MCSA)**

Mohamed Ali MOHAMED

**GRADUATE SCHOOL OF NATURAL AND APPLIED SCIENCE OF SELÇUK
UNIVERSITY
DEGREE OF MASTER OF SCIENCE
IN MECHATRONICS ENGINEERING**

Advisor: Assoc. Prof. Dr. Hayri ARABACI

2019, 59 Pages

Jury

Induction motors are the most used machines for electro-mechanical energy conversion due to their compactness and reliability. Despite the robustness, faults still occur in IM. Numerous works have been published but false diagnosis still remain an issue.

A machine learning approach for BRB detection is presented in this work. The approach used single-phase current measurements for detection of the faults. Sensing was performed using a hall-effect sensor. The signals were preprocessed and high frequency components removed. The signals were then amplified. An FFT algorithm was applied to convert the signals to frequency domain. Feature extraction and dimensionality reduction was carried out using principal component analysis (PCA). 24 samples were collected for each class under different load conditions.

2 classification schemes were proposed. Scheme 1 performs classification in one step and scheme 2 in 2 steps. Several experiments were performed to evaluate the systems developed. Key factors that were considered for the evaluation of the algorithms were overall classification accuracy, false positive and false negative rates. The effect of the number of principal components used on the performance was also inspected. With the proposed approaches, the rotor faults were classified with an error of 4.2%; and the faulty motors were diagnosed with 100% accuracy.

Keywords: induction motor, squirrel-cage, support vector machines, principal component analysis, fault detection, fault diagnosis, BRB, PCA, SVM.

ACKNOWLEDGEMENTS

Firstly, I would like to express utmost gratitude to my father, my mother and everyone in my family for their love, support, advice, sacrifice and patience throughout my life.

I would also like to thank my advisor, Dr. Hayri Arabacı, for his support, faith and advice throughout this research.

I reserve special thanks for my wife without whom I would not have gotten this far. I thank her for her love, care, understanding and undying support in all aspects of my life.



Mohamed Ali MOHAMED
KONYA-2019

TABLE OF CONTENTS

ÖZET	iv
ABSTRACT.....	v
ACKNOWLEDGEMENTS	vi
TABLE OF CONTENTS	vii
ABBREVIATIONS.....	ix
1. INTRODUCTION	1
2. INDUCTION MOTOR FAULTS.....	5
2.1. Induction Motor Faults	5
2.1.1. Stator Faults	5
2.1.2. Bearing Faults	5
2.1.3. Eccentricity-related Faults	5
2.1.4. Rotor Faults.....	6
2.2. Motor Current Signature Analysis (MCSA).....	6
2.3. Effect of Broken Rotor Bars on the Motor Current	7
3. FAULT DIAGNOSIS METHODS.....	9
3.1. Signature-based Methods.....	9
3.1.1. Classical Fast Fourier Transform.....	10
3.1.2. Wavelet Analysis	11
3.1.3. Park's Vector Approach.....	12
3.1.4. Hilbert Transform Method.....	13
3.1.5. Instantaneous Power FFT	14
3.1.6. Bispectrum	14
3.1.7. Statistical Parameters	15
3.2. Model-based methods	15
3.3. Knowledge-based methods	15
3.3.1.General Structure of the Knowledge-based methods	16
3.3.1.1 Principal Component Analysis (Feature Extraction)	17
3.3.2. Examples of Knowledge-based methods.....	17
3.3.2.1 Neural Networks	17
3.3.2.1 Support Vector Machines	19
4. MATERIALS AND METHODS	20
4.1. Data Acquisition, Signal Processing and Feature Extraction	20
4.2. Decision (Classification).....	21
4.2.1. Classification Scheme 1	21
4.2.2. Classification Scheme 2.....	23

5. EXPERIMENTAL SETUP	25
6. EXPERIMENTAL STUDY AND RESULTS	27
6.1. Data Acquisition, Signal Processing and Feature Extraction	27
6.2. Classification Results.....	33
6.2.1. Classification Scheme 1	33
6.2.2. Classification Scheme 2.....	38
7. DISCUSSION AND CONCLUSION	44
7.1 Discussion.....	44
7.2 Conclusion	44
REFERENCES.....	46
RESUME	50



ABBREVIATIONS

Abbreviations

ANN	: Artificial Neural Networks
FFT	: Fast Fourier Transform
kNN	: k Nearest Neighbor
PC	: Principal Component
PCA	: Principal Component Analysis
SVM	: Support Vector Machines
IM	: Induction motor
SIM	: Submersible Induction motor
MCSA	: Motor Current Signature Analysis



1. INTRODUCTION

Most of the conversion of electrical energy to mechanical energy is done by induction motors (IM). The machines are used widely domestically and in a variety of industries (Benbouzid ve Kliman, 2003). This is because they are compact, rugged and reliable (Taher ve Malekpour, 2011; Ojaghi ve ark., 2014). Despite being robust, faults occur due to some reasons that result from manufacturing errors or thermal, dynamic, environmental or mechanical stresses (Zhongming ve Bin, 2000; Abbaszadeh ve ark., 2001).

Failure of such machines could have important repercussions on the living things and the environment, so it is important to have early detection of faults in these machines so as to avoid unexpected failures, and lower the cost of maintenance (Matić ve ark., 2012). Unnecessary downtimes are also costly; and for this reason it is important to have condition-based maintenance (Taher ve Malekpour, 2011; Ojaghi ve ark., 2014). Furthermore, detection of faults during their inception is necessary so as to avoid the faults affecting other parts of the machine since a fault in one part of the machine may lead to more severe problems in another part. This phenomenon is known as ‘cascade sequence’ (Abbaszadeh ve ark., 2001).

The most reported IM faults can be broadly categorized into stator faults, bearing faults, eccentricity-related faults and rotor faults (Nandi ve ark., 2005). A myriad of papers have been published on detection of these faults. The main aim has been to develop an automatic online fault detection system that can overcome the challenges faced and give reliable diagnosis (Matić ve ark., 2012). The methods that have been presented in the literature for fault diagnosis in IM can be categorized into 3 main groups: signature-extraction based methods, model-based methods, and knowledge-based (machine learning) methods (Ali ve ark., 2018; Edomwandekhoe, 2018).

The signature-extraction based methods involve monitoring the motor parameters such as vibration, current, temperature etc. and checking for fault signatures in them. Vibration analysis (Su ve Chong, 2007), instantaneous power monitoring (De Angelo ve ark., 2010) and magnetic field analysis (Mirafzal ve Demerdash, 2005; Faiz ve ark., 2007) are examples of techniques that fall under this category.

Motor Current Signature Analysis (MCSA) and vibration analysis are the most popular techniques of this category (Benbouzid, 2000); however, monitoring the current has an advantage of remote-monitoring and being cheap while still providing same indication as the vibration analysis. Due to their high cost, vibration sensors are only reasonable to use in load-critical and expensive motors (Ghate ve Dudul, 2010).

The MCSA technique uses the stator current as the monitoring signal. Its advantage is simplicity in measuring it (Haji ve Toliyat, 2001), its non-invasiveness (Edomwandekhoe, 2018) and the inclusion of the current sensors in many motor drive systems for control.

One of the limitations of the signature-extraction based methods is that priori knowledge of the IM system is often required. For example, information on slip is needed for detection of BRBs from the side-band frequencies. Sometimes, this information is not available (Wang ve ark., 2012). Although in this case, parameter estimation can be used to get the slip, however this leads to highly complex computation (Ilonen ve ark., 2005).

The second category of the fault diagnosis methods (i.e Model-based methods) uses mathematical models that simulate the behavior of IMs when there is a fault. The algorithms under these category can provide warnings of faults; however its disadvantage is that the accuracy of diagnosis is depend heavily on the availability of explicit motor models (Ali ve ark., 2019). Examples of this approach are the works presented by (Ikeda ve Hiyama, 2007) for the detection of unbalanced voltage problem and (Arkan ve ark., 2005) for the simulation of stator inter-turn faults.

These traditional methods that fall under the first 2 categories can be expensive for practical implementation, difficult to use online, or require complex mathematical models. This led to the emergence of machine learning algorithms for fault diagnosis in IMs (Tan ve Huo, 2005).

The knowledge-based methods, trending in the field of fault diagnosis for the past 2 decades, detect faults by directly emulating the relationship between the inputs and outputs of the system paying little attention to the intermediate results (Liu ve Bazzi, 2017). First, the models are trained with inputs whose outputs are known. After

the training phase, the models are equipped with knowledge and are able to give diagnosis.

This group of algorithms has gained so much popularity among researchers recently and numerous papers have been published in the area. Machine learning algorithms such as Naive Bayes (NB), k-Nearest Neighbor (KNN), Support Vector Machines (SVM), Artificial Neural Network (ANN), Decision Trees have been successfully applied for fault diagnosis.

Bayes Theorem has been proposed by (Hajiaghajani ve ark., 2004) for detection of eccentricity-related faults in DC motors. NB, SVM and KNN algorithms have been used in (Wang ve ark., 2012) for the detection of stator, rotor and bearing faults. The KNN classifier has also been used in other instances: for the detection of BRB faults under varying mechanical loads (Ondel ve ark., 2006); and for detection of eccentricity-related faults (Ebrahimi ve ark., 2013). In the latter research work, fuzzy-SVM was used to give the severity of the faults. C4.5 and random forests have also been used for detection of bearing faults (Peng ve Chiang, 2011).

The most applied knowledge-based fault diagnosis algorithm has been ANN and hybrids of ANN owing to its desirable online application feature (Ali ve ark., 2019) and high accuracy (Palácios ve ark., 2015). Nonetheless, SVM is a method that stands out as well for several reasons like: high classification performance, less training time and good results with a small number of training data (Bacha ve ark., 2012). According to a study carried out by (Palácios ve ark., 2015) to compare different classifiers, SVM showed best performance judging by accuracy and processing time.

Feature extraction is an important aspect of any pattern recognition algorithm since the performance of the algorithm depends heavily on the features used. To be able to make an accurate diagnosis, the features should carry the fault information and should have adequate inter-class variation. Methods such as wavelet transform (Konar ve Chattopadhyay, 2011), Principal Component Analysis (PCA) and Linear Discriminant Analysis (LDA) (Peng ve Chiang, 2011) have appeared in the literature for feature extraction in fault diagnosis algorithms.

An interesting thing about the BRB faults is that they are degenerative, thus could result in IM failure and cannot be identified through inspection (Pezzani et al., 2018). Despite constituting only about 10% of the reported IM faults, majority of the research has focused on the detection of BRB faults. Still, false indications remain an issue and this area can be improved to ensure the industrial applicability of the solutions in the literature. Challenges that are faced include: BRB detection on low slip, sensitivity of classifiers to load intensity changes and sensitivity of classifiers to operating load conditions (Matić et al., 2012).

In this work, 2 fault diagnosis schemes are presented. The monitoring signal used is the motor current. FFT is performed on the current signals and analysis performed in frequency domain. Feature extraction is carried out using the PCA method and classification using SVM. Scheme 1 of the 2 proposed classification schemes, detects and classify the fault as per its severity in one go. The second scheme (scheme 2) does the same in 2 steps; the first step detects if there is a fault and step 2 gives the severity of the fault. Several SVM kernels are tested and the effect of the number of features used is inspected as well. Evaluation of the algorithms is in terms of the overall classification accuracy, classification accuracy for each severity level and true and false recognition rates.

The rest of the thesis is arranged as follows: Section 2 introduces different IM faults, MCSA and the effect of BRB on the motor current. Section 3 gives the general structure of fault detection algorithms, reviews the fault detection methods that appear in the literature and introduces the PCA algorithm. Section 4 gives the material and methods used in this work and section 5 provides the experimental setup. The experimental results are presented in section 6. The final part, section 7, contains the discussion and conclusion.

2. INDUCTION MOTOR FAULTS

2.1. Induction Motor Faults

Despite IM being robust and durable, faults are encountered due to some errors that may occur in the manufacturing phase or as a result of stresses from using the machine. The most commonly occurring faults in IM are (Nandi ve ark., 2005):

1. Stator faults
2. Bearing faults
3. Eccentricity-related faults
4. Rotor faults

2.1.1. Stator Faults

Stator faults, also referred to as armature faults, come about as a result of insulation defects that occur in the stator winding. They are brought about by either moisture, high temperature, system surge or faulty earth practices. The stator faults lead to asymmetry in the stator impedance by causing short circuits in the turns, windings and the stator body. Consequently, unbalanced phase currents are drawn by the motor. Stator faults account for 30-40% of the induction motor faults (Zhongming ve Bin, 2000; Haji ve Toliyat, 2001).

2.1.2. Bearing Faults

Accounting for about 50% of the reported induction motor faults, bearing faults occur as a result of mechanical stresses exerted on the bearing rings, raceways, balls or rolling elements. Bearing faults may occur due to fatigue despite the motor working under normal operating conditions with balanced loads and good alignment. Other causes of bearing faults are: contamination and corrosion, improper lubrication and improper installation of the bearings (Nandi ve ark., 2005).

2.1.3. Eccentricity-related Faults

Unequal air gap exists between the rotor and the stator. This condition is known as machine eccentricity (Heller ve Hamata, 1977; Cameron ve ark., 1986; Vas, 1993); and when it becomes large it leads to unbalanced radial forces which may cause the rotor and stator to be damaged (Nandi ve ark., 2005).

2.1.4. Rotor Faults

Broken rotor bars and end-ring faults make up 5-10% of induction motor faults. They arise from thermal stresses, magnetic stresses, residual stresses that arise from manufacturing faults, dynamic stresses, environmental stresses and mechanical stresses (Nandi ve ark., 2005). These faults can be classified into 3 categories (Arabacı ve Bilgin, 2010): high-resistance broken or cracked rotor bars or end-rings resulting into high resistance; poor connection (high resistance) between the rotor bars and the end-rings and short-circuit rotor laminas.

The squirrel-cage rotors in induction motors are of 2 kinds; cast (in motors with 3MW rating and lower) and fabricated (used in motors with higher ratings and special applications). Failure often occurs at the joints between the bars and the end-rings. Despite being more durable than fabricated cages, the cast rotors can hardly be repaired in the event of breakage (Matić ve ark., 2012).

It is important to detect broken rotor bars early because in this early stage, the torque characteristic changes are still not detected without measuring devices (Arabacı ve Bilgin, 2010).

2.2. Motor Current Signature Analysis (MCSA)

Motor parameters (for example, temperature, current, vibration etc.) can be used to determine if a motor is healthy or faulty. A comparison is made between the signals from the sensor of the motor being diagnosed and a reference measurement (Li ve ark., 2000).

Monitoring vibration and the stator current have been two of the most popular methods for induction motor fault diagnosis. However, it has been seen that monitoring the current has an advantage of remote-monitoring over vibration monitoring while providing the same indication (Kliman ve Stein, 1990; Kliman ve Stein, 1992; Benbouzid, 2000). Moreover, current sensors are easy to use and are included for

control purposes in many motor drive systems (Liu ve Bazzi, 2017). Also vibration sensors are more expensive and require sensitivity (Arabacı ve Bilgin, 2010).

MCSA has some limitations however. For example, the technique is not able to provide information on the configuration of non-contiguous BRBs when multiple broken bars exist in several parts of the rotor (Benbouzid ve Kliman, 2003). Furthermore, there are many factors that affect the current spectrum. Such factors include: electric supply, static load condition, dynamic load condition, noise and motor geometry (Benbouzid ve Kliman, 2003). These factors may lead to inaccurate diagnosis and false indications. The need for improvement in this aspect still remains present (Ali ve ark., 2019).

2.3. Effect of Broken Rotor Bars on the Motor Current

Broken rotor bars result in a magnetic field anomaly which produce spectral components in the motor current. These broken bar frequencies are given by equation (1) (Benbouzid, 2000)

$$f_{brb} = f_s \left[k \left(\frac{1-s}{p} \right) \right] \pm s \quad (1)$$

Where:

f_{brb} : the broken bar frequency

f_s : supply frequency

k/p : is equal to 1,5,7,11,13... according to the normal winding configuration

Despite the frequencies being the same for the BRB faults and eccentricity-related faults, the frequency corresponding to a particular harmonic number is different. This enables the two faults to be distinguished from each other (Benbouzid, 2000).

The condition of the motor can therefore be obtained through analysis of the stator current spectrum. The amplitude of the sideband frequency component is reflective of the number of broken bars available (Benbouzid, 2000; Benbouzid ve Kliman, 2003). The left side band (LSB) and the right side band (RSB) are calculated and used as features for fault detection.

With regards to the LSB values of the amplitude-frequency spectrum of a motor's phase current, some general conclusions have been drawn. These conclusions provide threshold values to classify motor rotor faults as follows (Matić *ve ark.*, 2012):

1. If the magnitude is -50dB or less, the rotor is healthy (Benbouzid, 2000).
2. If the magnitude is larger than -45dB, it implies that the rotor is faulty (Thomson *ve Fenger*, 2001).
3. For the magnitude values of between -54dB and -45dB, the '54–45 rule' proposed defines the values in this region as marginal (no reliable conclusion); for a magnitude less than -54dB, the rule declares the motor healthy; and for a magnitude larger than -45dB, there are BRBs according to the rule (Siau *ve ark.*, 2004).

However, these conclusions can only be made for nominal load conditions and cannot be drawn otherwise.

Furthermore, the magnitude of the LSB can also be used to give the number of BRBs present (Benbouzid, 2000; Matić *ve ark.*, 2012) as given by equation (2):

$$\frac{I_{brb}}{I_s} \cong \frac{\sin \alpha}{2p(2\pi - \alpha)} \quad (2)$$

Where:

$$\alpha = \frac{2\pi R_b p}{R}$$

I_s is the stator current fundamental frequency component

R_b is the number of broken bars present

I_{brb} is amplitude of LSB frequency component $f_s(1 - 2s)$

Additionally, the RSB component, $f_s(1+2s)$, can also be used to give a severity diagnosis of the faults (Benbouzid, 2000).

3. FAULT DIAGNOSIS METHODS

The technological advancement in the field of computerized data acquisition and digital data processing led to development of a multitude of techniques for fault detection and condition diagnosis techniques of IMs. The methods can be roughly categorized into (Edomwandekhoe, 2018):

1. Signature-based methods
2. Model-based Methods
3. Knowledge-based Methods

3.1. Signature-based Methods

These techniques involved the use of spectral analysis of operational process parameters like temperature, pressure, current, vibration etc. Signature-based methods take form in one or a combination of the following:

1. Time domain analysis
2. Frequency domain analysis

Time-domain methods are applied by monitoring the changes of machine features with time. They involve simpler calculations but they usually have a lower sensitivity to faults. For this reason, they tend to have difficulty in identifying incipient faults or in fault detection in noisy environments. Frequency-domain methods on the other hand are implemented by analyzing various spectra since machine faults generate additional spectral components. The methods include FFT, instantaneous power FFT, FFT on extended Park's vector etc. (Liu ve Bazzi, 2017).

Below, we review some of the signature-based stator current monitoring techniques that are presented in the literature. The method discussed are:

1. Classical Fast Fourier Transform
2. Instantaneous Power FFT
3. Park's vector approach
4. Bispectrum
5. Wavelet Analysis

3.1.1. Classical Fast Fourier Transform

One popular approach used to analyze the motor current for fault detection is the FFT approach. In the case of BRB faults, equation (3) gives the BRB frequencies in the motor current (Kliman ve Stein, 1992).

$$f_{brb} = [1 \pm 2ks]f_s \quad (3)$$

Where:

$$k = 1, 2, 3, \dots$$

f_s : electrical supply frequency,

s : the slip

In order to calculate the slip, information on the speed is required. This can either be obtained using an encoder or otherwise it can be estimated (Matić ve ark., 2012).

The classical fourier transform technique constitutes 4 main stages: sampling, pre-processing, fault detection and post-processing (Benbouzid, 2000).

Sensing is firstly carried out through a current transformer. In the sampling stage, the excitation component (50Hz) is removed from the single-phase motor current through the use of a low-pass filter (50Hz notch filter). This removes the undesired high frequency components (which produce an aliasing effect in the sampled frequency). The signal is then amplified so as to maximize the use of the input range of the AC/DC converter. The filtered current is then sampled by the AC/DC converter at a predetermined sampling rate (multiple of 50 HZ) over a sufficient sampling period to obtain the needed FFT.

Pre-processing involves converting the sampled signal into frequency domain through the use of an FFT algorithm. The result is a generated spectrum containing the magnitude of each frequency spectrum. De-noising is also carried out in this stage.

Fault detection is what follows. In this stage, a frequency filter is used to remove the frequency components that contain no useful information associated with the faults.

The fault detection algorithm specifies characteristic frequencies associated to particular faults thus retaining the components of interest.

The work of the post-processor is to diagnose the frequency components and classify them into specified faults.

There are some drawbacks associated with the use of the MCSA-based FFT for industrial settings. The method cannot be reliable for rotor fault detection at low slip. The difficulty of using the MCSA method practically is related to the following (Matić ve ark., 2012):

1. Restricted time window resulting in spectral leakage
2. Need for high frequency resolution.
3. Varying load conditions.
4. Confusing mechanical frequencies that cause ambiguity.

Envelope analysis methods like Park's vector approach and Hilbert transform have been used to overcome these problems (Saddam ve ark., 2018).

3.1.2. Wavelet Analysis

The usefulness of fourier transform is limited to stationary signals. As a solution for this challenge so as to make it suitable for transient signals, it was adapted to analyze a small part of the signal at a given time in a technique referred to as short-time Fourier transform (STFT). The technique, also known as windowing technique, maps a signal into a function of time and frequency, providing information on the two (Benbouzid, 2000).

Nonetheless, STFT provides information with limited precision dependent on the fixed size of the window. To overcome this drawback, the wavelet transform method was introduced. Using a variable-size window, the wavelet analysis method allows using long time intervals where more precise low-frequency information is desired and shorter windows for high-frequency information (Benbouzid, 2000).

In the context of fault diagnosis, the wavelet analysis method has been used in many applications owing to its ability to perform analysis of stator current signals in transient state.

3.1.3. Park's Vector Approach

Three-phase induction motor phenomena can be described using stator current Park's vector introduced in (Cardoso ve ark., 1999). The components (i_d and i_q) of the Park's vector are given as a function of mains phase variables (i_a , i_b and i_c) as described in equation (4):

$$\begin{cases} i_d = \sqrt{\frac{2}{3}}i_a - \frac{1}{\sqrt{6}}i_b - \frac{1}{\sqrt{6}}i_c \\ i_q = \frac{1}{\sqrt{2}}i_b - \frac{1}{\sqrt{2}}i_c \end{cases} \quad (4)$$

Ideally the components of the park's vector are as follows (equation (5)):

$$\begin{cases} i_d = \frac{\sqrt{6}}{2}i_M \sin \omega t \\ i_q = \frac{\sqrt{6}}{2}i_M \sin \left(\omega t - \frac{\pi}{2} \right) \end{cases} \quad (5)$$

Where:

i_M is the maximum phase value of the supply current

ωt is the supply frequency

The park's vector is represented as a circular pattern with its center at the origin of the coordinates. The technique can be used for fault detection by monitoring deviations in the acquired pattern.

The induction motor supply current contains additional sideband components when there are BRB faults. The additional components are available in the motor current as well as the Park's vector components i_d and i_q . Therefore, in this situation, it is seen that the spectrum of the stator current Park's vector modulus is the sum of a dc level, which is generated by the fundamental component of the supply current, plus two additional terms, at frequencies of 2sfs and 4sfs. So, the spectrum of the current Park's

vector modulus ac level is clear from any component at the fundamental supply frequency. This make it useful in detecting components related to the fault. This use of this technique aimed to counter the problems faced in traditional MCSA (MA Cruz, 2000).

This method is a popular time-domain technique which can be used to give the severity of the fault. However the technique cannot differentiate between the types of faults and requires the use of 3 current sensors (Liu ve Bazzi, 2017).

3.1.4. Hilbert Transform Method

The FFT approach has some drawbacks in detecting some faults (refer to Classical Fourier approach), especially with motors performing under no load or low-load conditions. The Hilbert transform technique counters these problems and the approach has been applied successfully to detect the BRB-related frequencies even at low slip (Puche-Panadero ve ark., 2009a; Puche-Panadero ve ark., 2009b).

The following equations (6), (7) and (8) give the foundation of Hilbert transform (Saddam ve ark., 2018):

$$HT(x(t)) = I(t) = \frac{1}{\pi} \int_{-\infty}^{+\infty} \frac{x(\tau)}{t-\tau} d\tau \quad (6)$$

$$z(t) = x(t) + j.I(t) \quad (7)$$

$$\begin{cases} A_z(t) = \sqrt{x(t)^2 + I(t)^2} \\ \phi_z(t) = \arctan\left(\frac{x(t)}{I(t)}\right) \end{cases} \quad (8)$$

Where:

$HT(x(t))$ is the Hilbert transform of signal $x(t)$

$z(t)$ is the analytic created from the studied signal and it Hilbert transform

$A_z(t)$ is the amplitude of $z(t)$

$\phi_z(t)$ is the instantaneous phase of $z(t)$

3.1.5. Instantaneous Power FFT

The instantaneous power is a product of the supply voltage and the motor current. It has been shown that it may also be used as a substitute for the motor current as a signature analysis technique for fault detection in induction motors. It contains more information than using just the current, as it has one more component at the modulation frequency. It also has another advantage in that the fault harmonics domain is well-bounded due to the translation of the fault harmonics into the '0-100 Hz' frequency band.

Despite the advantages of using this technique, the power spectra are noisy, hence the technique does not result in significant improvement thus the motor current remains the main means of motor signature analysis (Maier, 1992; Legowski ve ark., 1996; Trzynadlowski ve ark., 1999; Benbouzid, 2000).

3.1.6. Bispectrum

Consider $x(k)$ to be a stochastic signal with zero mean, k to be the time index, and τ_1 and τ_2 as lag variables. Then the third-order moment (in time domain) of $x(k)$ is given in equation (9) , and its bispectrum (in frequency domain) in equation (10) (Benbouzid, 2000).

$$c_{3,x}(\tau_1, \tau_2) = E(x(k), x(k + \tau_1), x(k + \tau_2)) \quad (9)$$

$$C(\omega_1, \omega_2) = \sum_{\tau_1=-\infty}^{+\infty} \sum_{\tau_2=-\infty}^{+\infty} c_{3,x}(\tau_1, \tau_2) \exp\{-j(\omega_1\tau_1 + \omega_2\tau_2)\} \quad (10)$$

It is evident from equation (10) that the bispectrum can provide information on the amplitude and phase of the signals. This additional information can bring about enhancement in fault diagnosis (Chow ve Fei, 1995).

It has been seen through experimental results that the bispectrum magnitude of the dominant component increases as the level of the fault increases, confirming that this method can provide enough spectral information for condition diagnosis of induction motors with particular importance in electrical-based faults (for example, stator voltage unbalance). This is because such faults lack a well distinguished harmonic frequency component (Benbouzid ve ark., 1999; Benbouzid, 2000).

3.1.7. Statistical Parameters

BRBs produce a change in the statistical behavior of the current signal and several methods have been used for the detection of the faults by analyzing these changes. In (Matić *ve ark.*, 2012), skewness and kurtosis were applied on the current signal and its envelope in time domain for the detection of BRBs. The envelope of the signal is obtained using Hilbert transform.

3.2. Model-based methods

These methods involve predicting the behavior of the IM in the presence of fault using mathematical models. Computer simulation has been seen to be a useful tool that can be used to provide insight into the dynamic behavior and electro-mechanical interaction of machines; and using a suitable model, faults as well as changes in the corresponding parameters can be simulated (Liang *ve ark.*, 2002).

Examples of this approach are the works presented by (Ikeda *ve Hiyama*, 2007) for the detection of unbalanced voltage problem and (Arkan *ve ark.*, 2005) for the simulation of stator inter-turn faults. Asymmetric stator and rotor faults have been successfully simulated in the works published by (Liang *ve ark.*, 2002)

Despite being able to provide the diagnosis, the demerit is that the accuracy of these methods depend heavily on the availability of explicit motor models (Ali *ve ark.*, 2019).

3.3. Knowledge-based methods

The machine learning approach is a relatively new trend that has been successful in modelling non-linear systems through directly emulating the relationship between the inputs and outputs without giving much attention to the physical structure and intermediate results of the system (Liu *ve Bazzi*, 2017).

The advantage of these methods is that trigger thresholds, machine models or even the load and motor characteristics are not required (Ali *ve ark.*, 2019).

The methods include: Neural Networks (NN), Support vector machines (SVM), Decision Trees, k-nearest neighbors (KNN) etc.

3.3.1. General Structure of the Knowledge-based methods

The flowchart in figure 3.3.1 gives the general design of knowledge-based fault diagnosis algorithms. The algorithms are carried in 2 phases: training and diagnosis.

In the training phase, the motor measurements are acquired, processed and then the features extracted. These features are used to train the intelligent models and equip them with knowledge to make the diagnosis.

After the training phase is completed, new measurements from the motor to be diagnosed are taken and used as input for the trained model. In this stage the trained model gives the diagnosis.

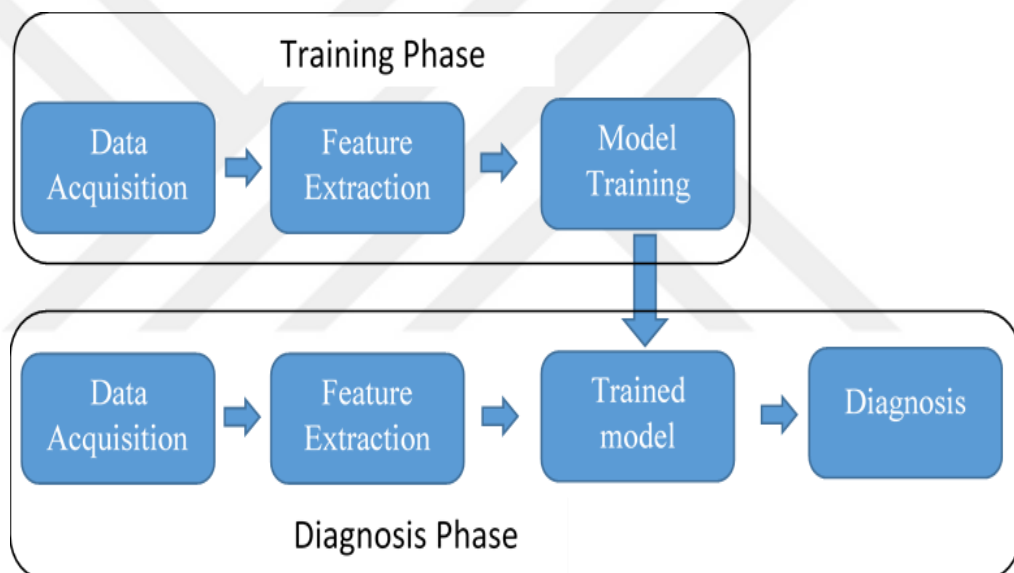


Figure 3.3.1: General structure of knowledge based methods

The most commonly used motor signal for knowledge-based methods is the current signal. It can either be used on its own or combined with other signals like vibration, winding and bearing temperatures or other motor parameters (Ali ve ark., 2019).

The performance of the algorithms depends majorly on the features extracted. In the literature several feature extraction techniques have been used to obtain the fault indicators found in the mechanical and electrical signals. Such techniques include spectrum analysis, statistic feature extraction etc. (Liu ve ark., 2018).

3.3.1.1 Principal Component Analysis (Feature Extraction)

Introduced in 1901 by Karl Pearson (Pearson, 1901), the PCA algorithm has been used widely in many different industries in Engineering and Economics (Martins ve ark., 2007). Researchers have employed the technique for feature extraction in pattern recognition applications. The main idea of PCA is projecting high-dimensional data to lower dimensional data while retaining the information by preserving features that have higher variance (Ozgonenel ve Yalcin, 2010).

Many times, features are related to each other, and PCA expresses these features as a linear combination of new features transforming correlated features into uncorrelated features known as principal components. Commonly used in face recognition and image compression applications, PCA has also been applied in fault detection (Peng ve Chiang, 2011).

The steps of PCA involve creating a training matrix from the training data, then finding the covariance of the matrix. The eigenvectors and eigenvalues of this covariance matrix are then computed and arranged in descending order. The number of principal components to be extracted is then selected and the projection matrix built. This is used to project the input samples into the PCA feature space (Barnouti ve ark., 2016).

3.3.2. Examples of Knowledge-based methods

3.3.2.1 Neural Networks

Artificial neural networks (ANN) are inspired by the biological neural networks. Their building blocks are processing units known as neurons. The neurons interact with one another by sending signals along weighted connections. With their ability to copy human expertise, which makes them suitable in handling non-linear systems, their function is to give an output decision based on the input values.

The ANNs are firstly trained using a set of training data that provides the input/output map. At first the neural networks give inaccurate output results. An error quantity is measured and used to modify the connections between the neurons. The process is repeated, modifying the strength of the connections until the desired activation function is achieved. After training, the system has a knowledge

representation that can accurately identify the faults (Li ve ark., 2000; Arabacı ve Bilgin, 2010).

Many papers have been published proposing ANN and hybrid ANN algorithms (combining ANN with other methods) for fault diagnosis. The proposed ANN algorithms use different learning procedures, features and methods of feature selection etc. and have been used for the detection of different types of IM faults.

In (Li ve ark., 2000), neural networks have been used to detect bearing faults using vibration signals features in time and frequency domain as the inputs.

In the research carried out by Hua Su and Kil To Chong (Su ve Chong, 2007), STFT was performed on vibration signals in the quasi-steady state to extract the features for the ANN. The developed scheme was successful in detecting BRB faults as well as eccentricity faults.

In the work presented in (Ayhan ve ark., 2006), ANN algorithms were developed to detect BRB faults under different load conditions. The experimental results of the experiments showed ANN performed better than Multiple Discriminant Analysis (MDA) it was being compared with.

The authors in (Bossio ve ark., 2013) presented neural network schemes which employ self-organizing maps for fault diagnosis in IMs. They successfully identify load unbalance and shaft misalignment faults using one of the scheme and classify broken rotor bars and oscillating load faults using the other.

The study carried out in (Ertunc ve ark., 2013) used ANN and Neuro-Fuzzy (ANFIS) models to give a diagnosis of the bearings in an induction motor. Analysis in the work was performed on the vibration and stator current in the time and frequency domains.

Hybrid machine learning models that used Neural Network Fuzzy Min-Max (FMM) and Random Forest classifiers have been used to monitor the condition of induction motors (Seera ve ark., 2014). In the study the experiments were performed under 25%, 50%, 75% and nominal torque. The inputs of the system were obtained through the MCSA method from the stator current.

3.3.2.1 Support Vector Machines

Support Vector Machines are a machine learning algorithm that are based on statistical learning. They were initially developed as a solution for binary classification. Two linearly separable classes can be separated by several linear classifiers referred to as hyper-planes; however one of the hyper-planes is able to perform maximum separation. This hyper-plane is known as the maximum separating hyper-plane and has the maximum margin. The margin is the distance between a hyperplane and the nearest data point of each class. The aim of SVMs is to create an optimal hyperplane. The data points that lie either on or within the margin are called support vectors (Vapnik et al., 1994).

In the case of the data not being linearly separable, an appropriate kernel function is used to map the data into a higher dimensional feature space where it becomes linearly separable; then constructing the hyperplane to separate the data classes (Afifi, 2014; Gangsar et al., 2017). The types of kernel functions are Linear, Polynomial and Gaussian radial basis function (RBF) (Ali et al., 2018).

SVMs stand out due to their high classification performance, less training time and the ability to give good results in cases of a small number of training data (Bacha et al., 2012). The research performed in (Palacios et al., 2015) which evaluates these methods shows that Artificial Neural Networks with multilayer perceptron (ANN/MLP) has given accuracies of more than 99.7% for the detection of broken rotor bar faults. Experiments performed for bearing faults indicate that SVMs are accurate and robust and have the best performance judging by their accuracy and processing time.

4. MATERIALS AND METHODS

Although there exist some small differences in the structures of traditional Induction motors (IMs) and Submersible Induction motors (SIMs), they essentially use the same working principle. The main differences are in the diameters of the motors, the length of the rotors, the material used and the manufacturing processes of the two types of motors.

The diameter of the wells pose a size constraint when it comes to submersible motors. For this reason, SIMs tend to have smaller diameters compared to the traditional IMs. To compensate for the small diameters and to increase motor power, submersible IMs are made longer. The bars and end-rings of the conventional IMs are made from aluminium casting whereas these parts in submersible induction motors are made of copper bar and plate. The bars and plate are then connected through welding.

The welded regions are prone to faults that result from mistakes that may have occurred in the manufacturing process or later due to the stresses exerted on the motor. This could result in poor conductivity in the rotor bars and end-rings; thus causing current not to flow. These faults are what are termed as ‘broken rotor bar’ faults.

The supply current of the IM can be used as the monitoring signal to detect broken rotor bars. Several feature extraction techniques have been used to obtain the fault indicators. The fault diagnosis methods in this study are divided into three main sections: data acquisition, feature extraction and decision (Classification). Experimental data was used to develop the machine learning system to detect and classify rotor bar faults in induction motors according to their severity.

4.1. Data Acquisition, Signal Processing and Feature Extraction

The signals were obtained using hall-effect current sensors. The current signals acquired were processed and analysed in the frequency domain. The transformation was performed using Fast Fourier transform (FFT). A total of 24 samples was collected for each of the 5 studied classes; giving a total of 120 samples. PCA transformation was then performed on the current signals in frequency domain for feature extraction and dimensionality reduction. Figure 4.1 shows the flowchart of the data acquisition, signal processing and feature extraction process. To find the optimal number of principal components to use, the first 2, 5, 10, 20, 30, 40, 50, 60, 70, 80, 90 and 100 principal

components were extracted to create the feature vectors and stored in a database. These were used separately as the inputs for the classifiers in the experiments carried to train and test the different classifiers studied.

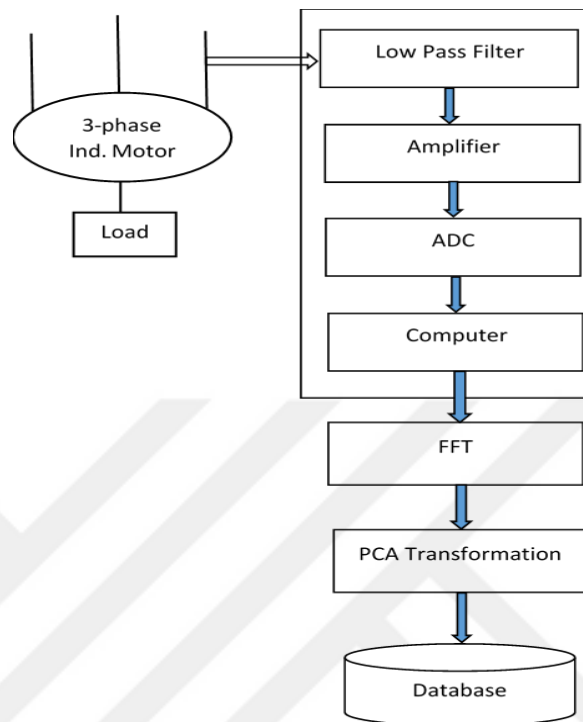


Figure 4.1 : Flowchart for Data Acquisition, Signal Processing and Feature Extraction

4.2. Decision (Classification)

For classification, SVM with different kernel functions were used in several experiments carried out. The SVM kernel functions studied were: Linear, Quadratic, Cubic, Fine Gaussian, Medium Gaussian and Coarse Gaussian. Two classification schemes were proposed and their performance compared.

4.2.1. Classification Scheme 1

The first scheme directly classified the input sample into one of the five studied classes: healthy, 1 BRB, 2 BRB, 3 BRB or half-BRB. The database used to train and test this method contained 24 samples from each class. A 5-fold cross validation method was used to evaluate the performance of each classifier studied. Figure 4.2.1.a shows

the flow chart of the technique used in scheme 1. Figure 4.2.1.b gives the flowchart of the experiments performed for the evaluation of this technique.

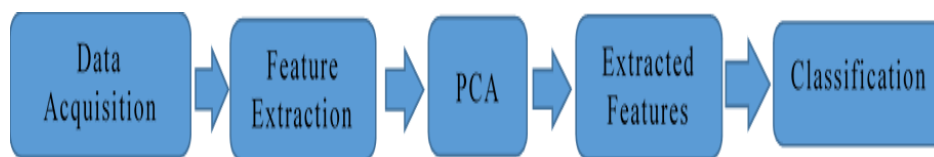


Figure 4.2.1.a: Flowchart for the proposed 'scheme 1'

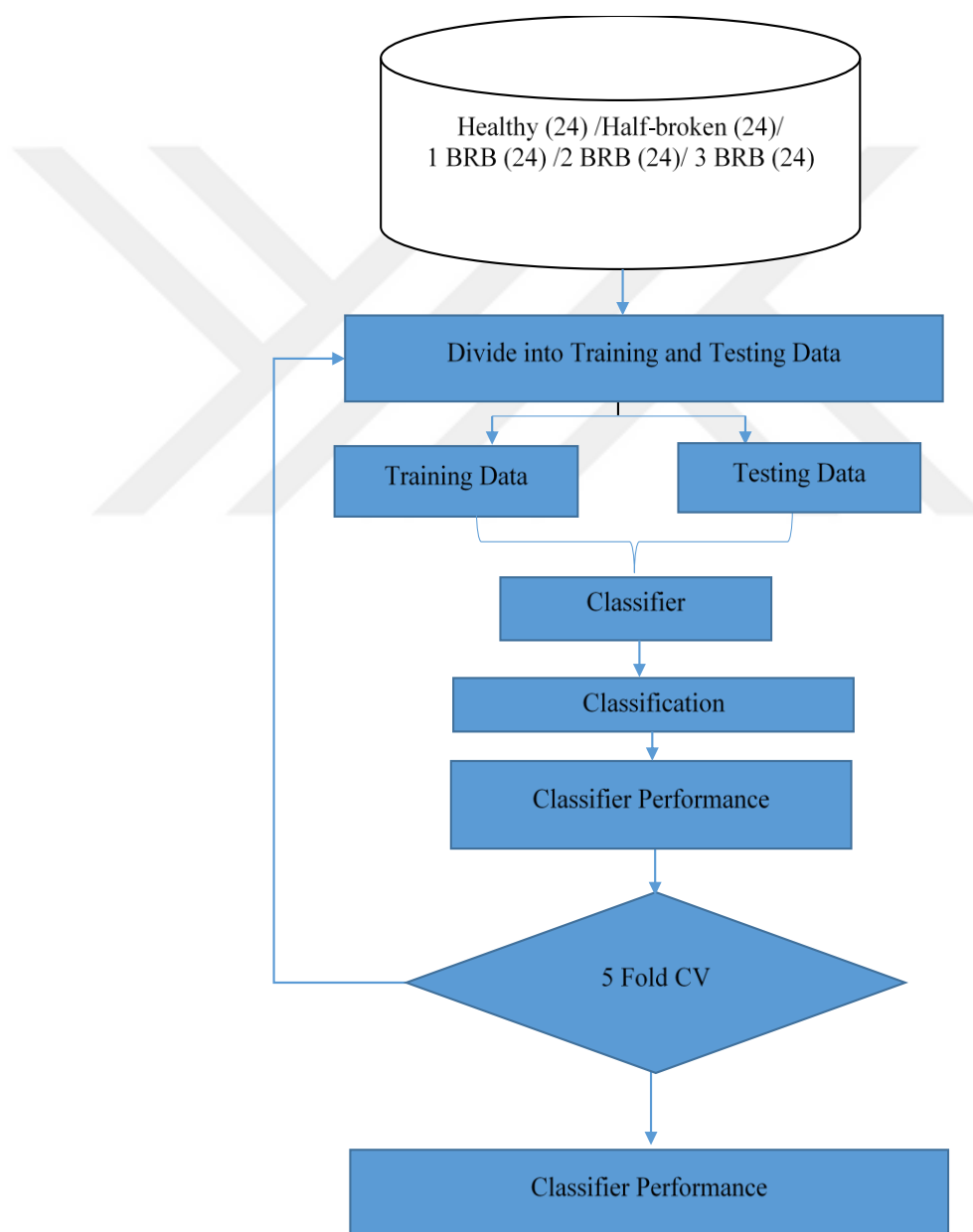


Figure 4.2.1.b: Flowchart for the experiment to evaluate 'scheme 1'

4.2.2. Classification Scheme 2

In the second scheme, classification was performed in 2 steps; the first step determined if the motor was healthy or faulty and the second step determined the severity of the fault as shown in the Figure 4.2.2.

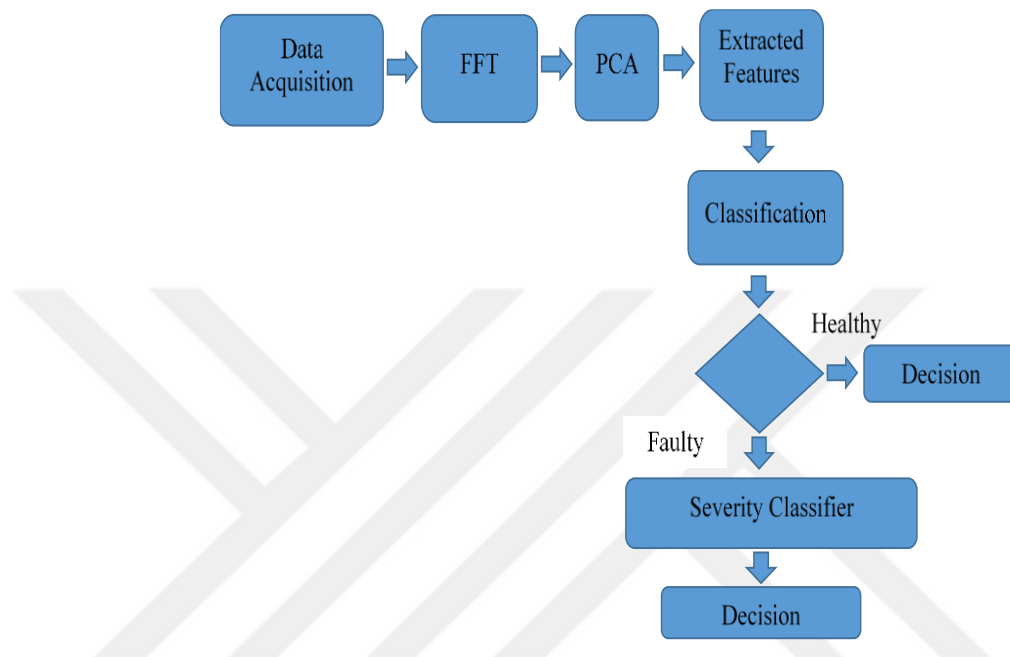


Figure 4.2.2: Flowchart of the proposed 'Scheme 2'

Step 1: Is the motor healthy or faulty?

In the first step of scheme 2, after the current was measured, the signal processed and the features were extracted, the classifier was used to classify it into either being healthy or faulty.

To test the performance of the classifiers used in the first step, the experiment described by the flowchart in figure 4.2.2.1 was performed. In the experiments, the data was divided into 4 datasets each containing all the 24 samples of the 'healthy' class and 6 samples from each of the 4 studied faults so as to have an equal number of samples for the two classes. The samples of the 'faulty' class contained in each dataset was different, so as to provide a more accurate behaviour of the system under different conditions.

5-fold cross validation method was used to test each classifier and the accuracy of fault detection recorded. To evaluate this step in the proposed algorithm, the overall accuracy was calculated by averaging the individual accuracies of using the 4 datasets.

Step 2: If the motor is faulty, what is the severity?

For the second step, only samples from the faulty motors were considered as the aim of this step was to classify the fault by its severity.

To test the performance of the classifiers in performing this step, 24 samples from each of the faulty conditions were used to create the database. 5-fold cross validation method was used to evaluate the performance of the classifiers studied. To evaluate this step in the proposed algorithm, the overall accuracy was calculated by averaging the individual accuracies of using the 4 datasets.

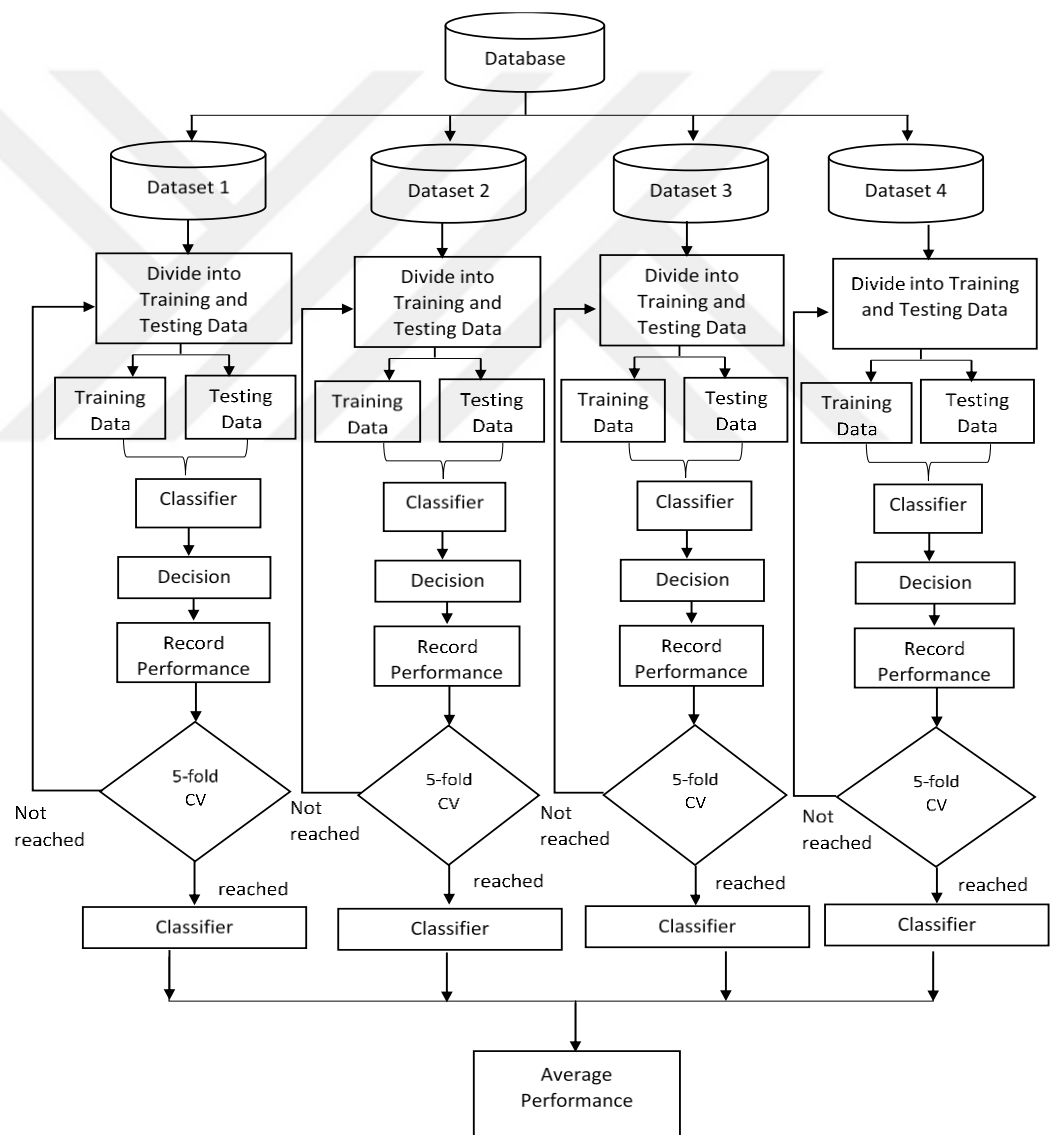


Figure 4.2.2.1: Experiments to evaluate step 1 of 'Scheme 2'

5. EXPERIMENTAL SETUP

The experiments in this study were performed in a SIM factory using a motor-generator system. Motor loading was performed using a generator and levelling of the load was carried out through resistors conducting to the generator. Figure 5 shows the pictures taken of the experimental setup.

The squirrel-cage motors used to perform these experiments had the following specifications:

- Power: 25 HP
- Number of bars: 22
- Rotor diameter: 71 mm
- Bar diameter: 6.1 mm
- Stator diameter: 72 mm
- Rotor length: 520 mm



Figure 5: Experimental setup picture

The broken rotor faults were simulated at the factory during the production stage; and with the aim of ensuring that accurate measurements were recorded, the faults were fabricated separately. That is, five different motors were used for the five studied classes. Creating the broken bar faults involved drilling through the middle section of the motor bars thus reducing the conductivity of the bar or making it zero

therefore high resistance. The half broken bar fault was simulated by drilling until half-way through the bar giving the effect of reduced conductivity; thus also high resistance. This half-bar fault represents the incipient stages of a BRB fault.

The simulated faults were as listed below:

- One broken bar
- Two broken bars
- Three broken bars
- A half broken bar



6. EXPERIMENTAL STUDY AND RESULTS

6.1. Data Acquisition, Signal Processing and Feature Extraction

Sampling of the single-phase current was performed using a hall-effect sensor. A low-pass filter was then used on the analog signal to remove the undesirable high frequency components. Then, the signal underwent amplification and in turn maximizing the use of the analog-to-digital converter (ADC) input range; which sampled the filtered current signal at a predetermined sampling rate of 7.5KHz. Figures 6.1.a (1-5) show the current signals sampled from a healthy motor and motors with different rotor faults under the same load conditions.

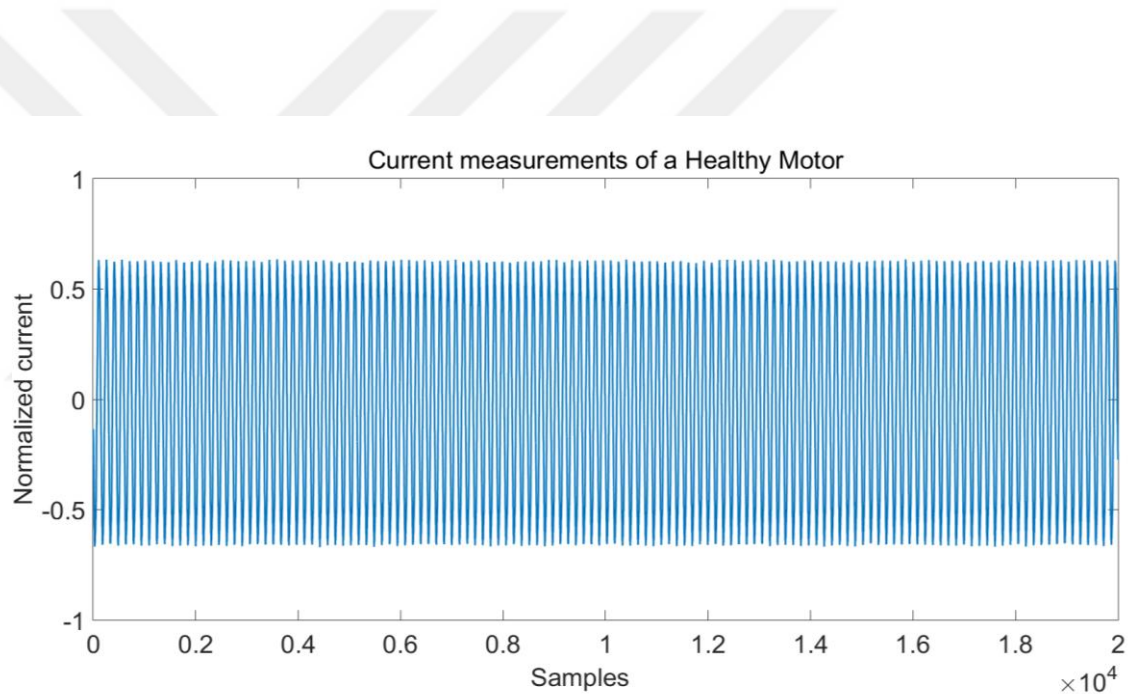


Figure 6.1.a.1: Current of a healthy motor

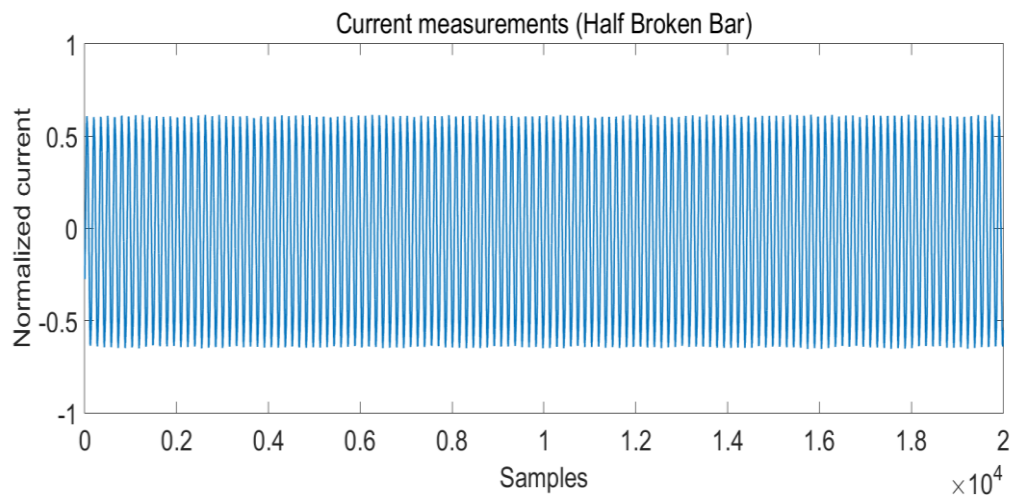


Figure 6.1.a.2: Current of a motor with a half broken bar

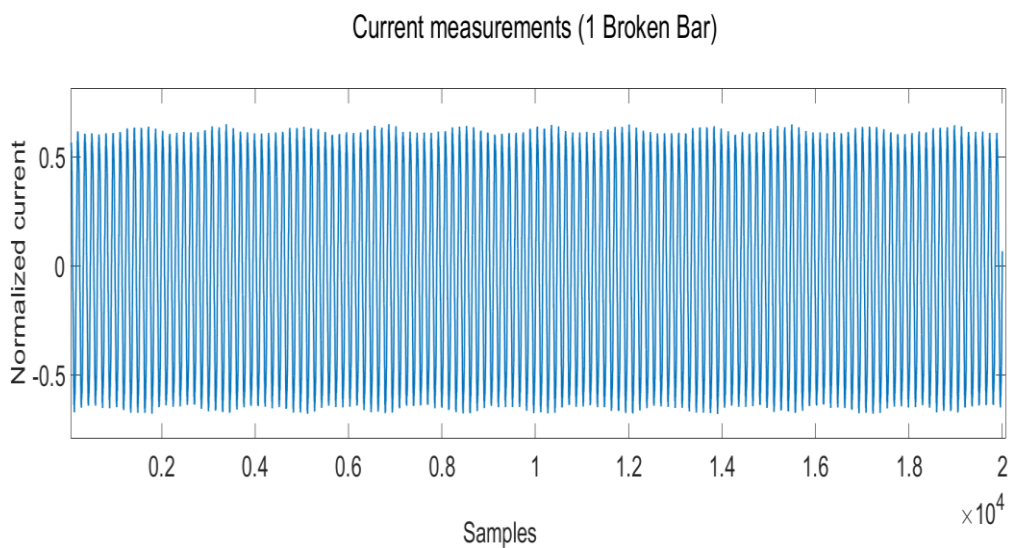


Figure Figure 6.1.a.3: Current of a motor with one broken bar

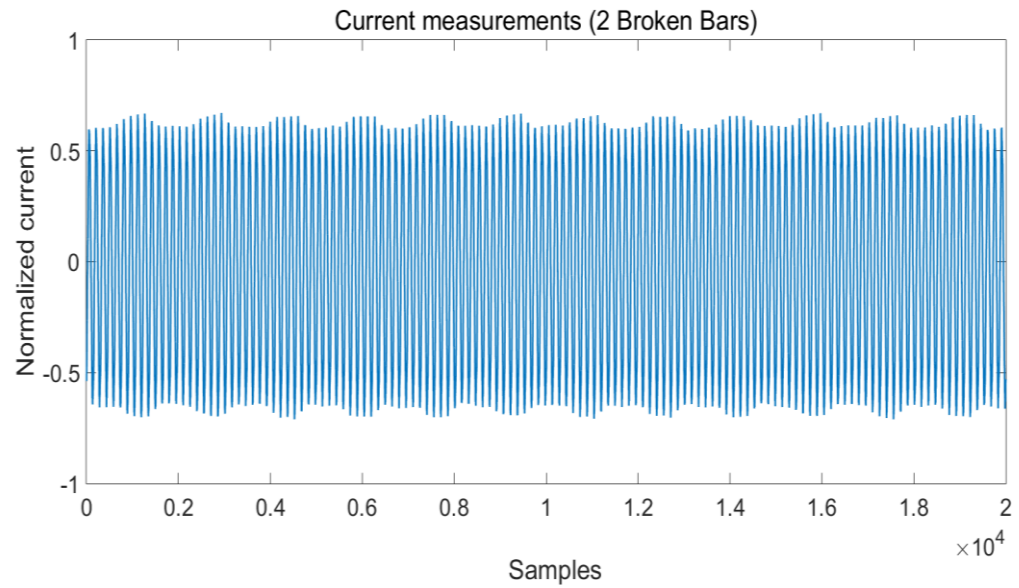


Figure 6.1.a.4: Current of a motor with two broken bars

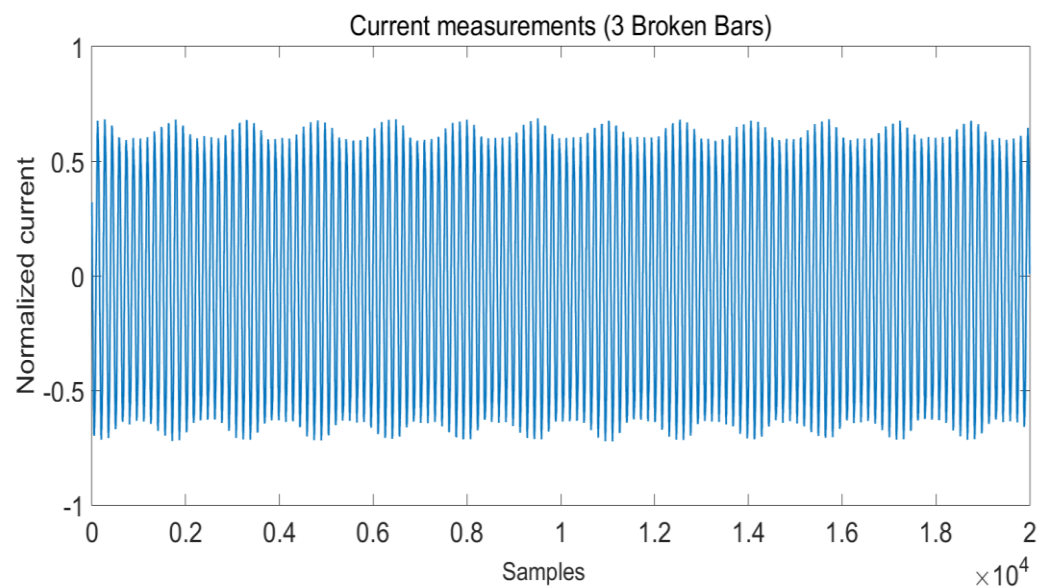


Figure 6.1.a.5: Current of a motor with three broken bars

Fast Fourier transform was then performed on the current signals and analysis performed in the frequency domain. Figures 6.1.b (1-4) show a comparison between the amplitude of power spectra of the current of a healthy motor and that of motors with the studied broken rotor bar faults under the same load conditions.

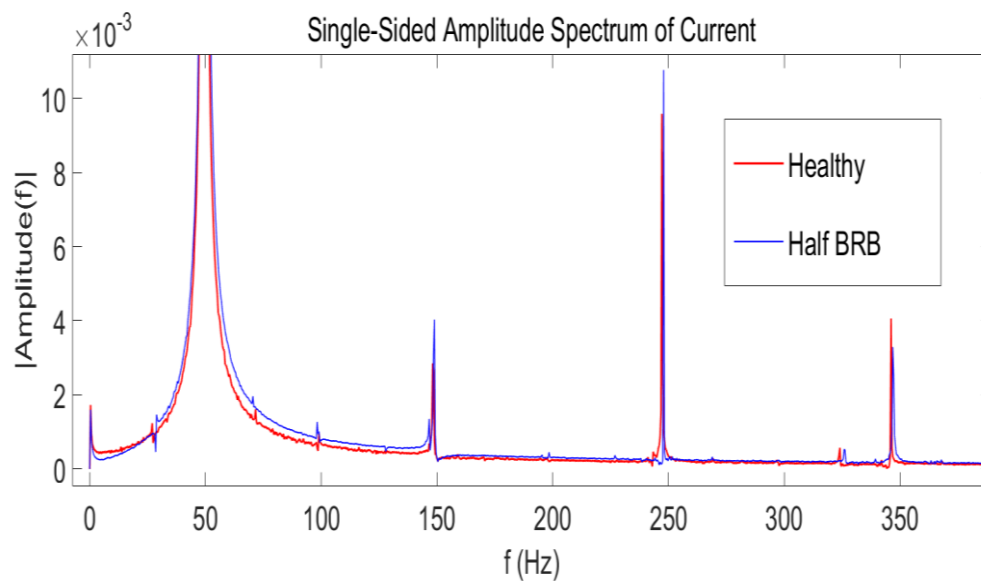


Figure 6.1.b.1: Comparison of the amplitude of power spectra (Healthy vs Half broken bar)

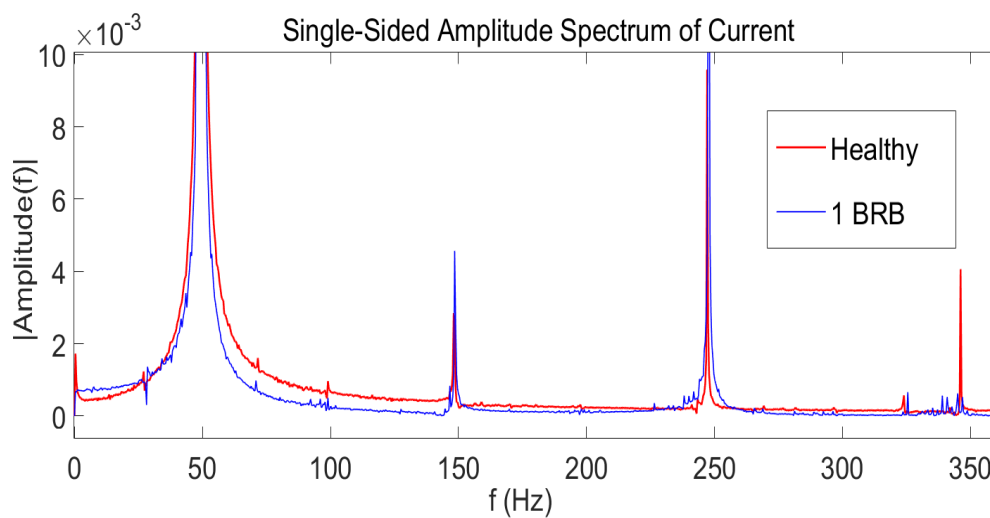


Figure 6.1.b.2: Comparison of the amplitude of power spectra (Healthy vs 1 broken bar)

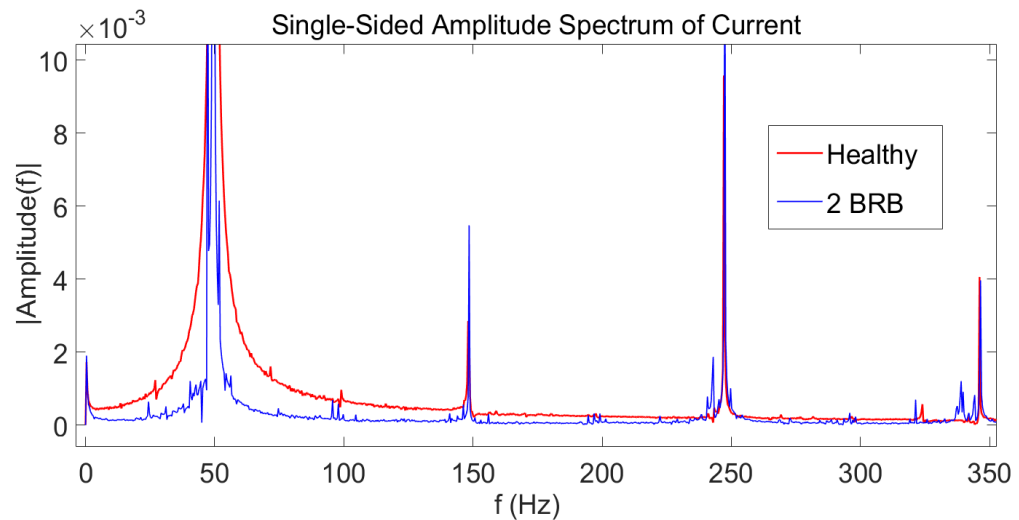


Figure 6.1.b.3: Comparison of the amplitude of power spectra (Healthy vs 2 broken bars)

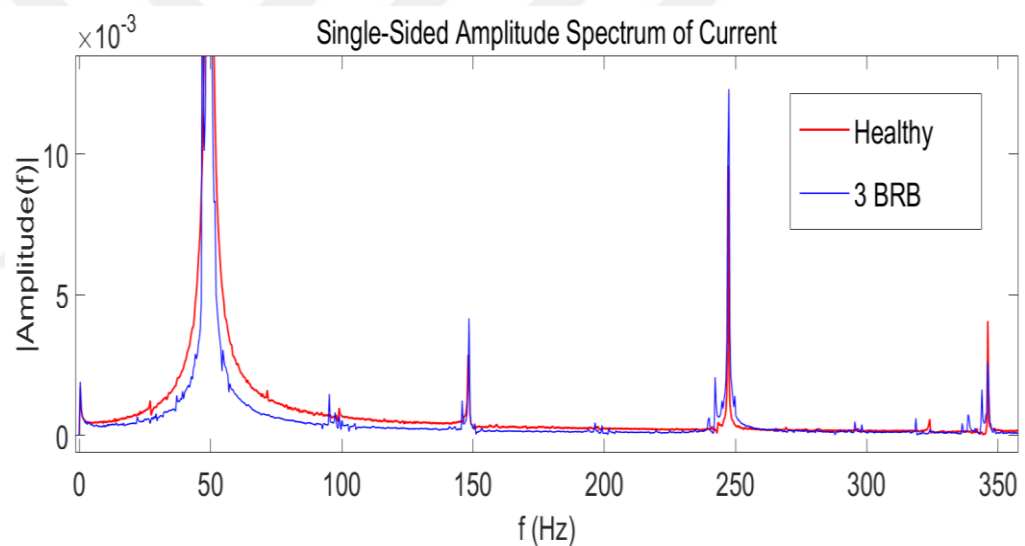


Figure 6.1.b.4: Comparison of the amplitude of power spectra (Healthy vs 3 broken bars)

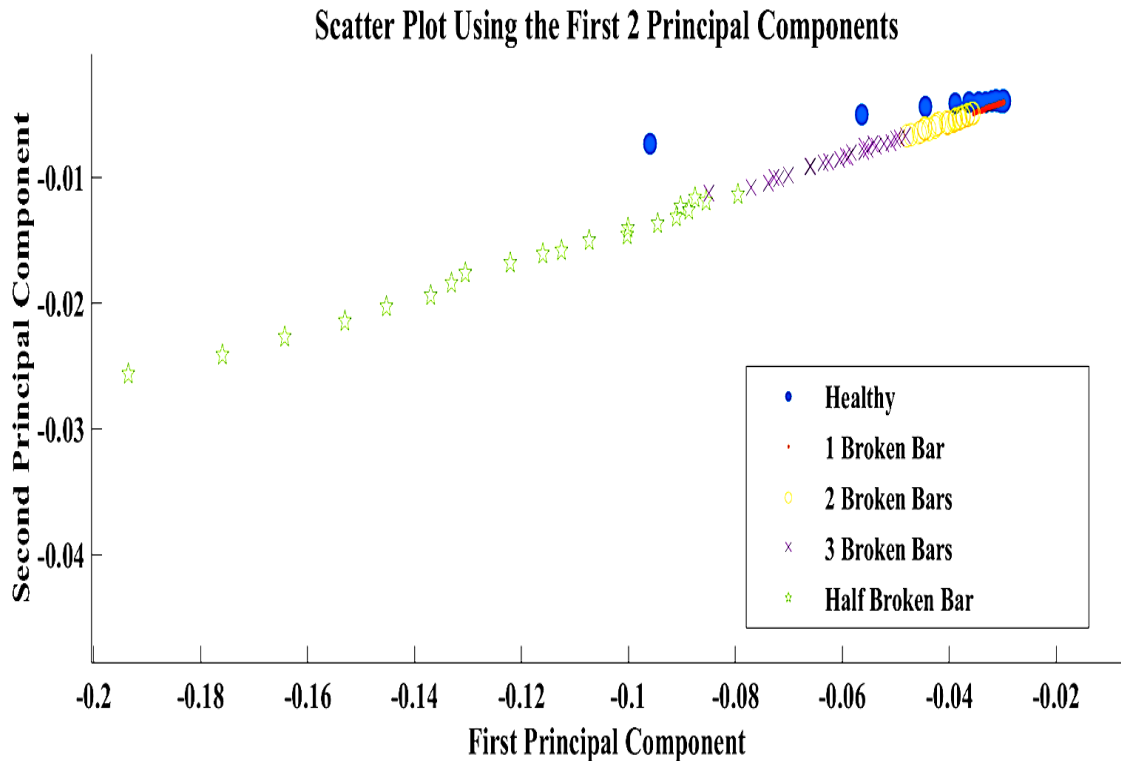
Feature Extraction (PCA) results

There was a total of 120 samples (24 samples per studied condition) used in this study, and each sample of the data was a 10,001 by 1 matrix at this point. Principle Component Analysis was used for feature extraction and dimensionality reduction and was performed as in the steps described below:

1. The samples were concatenated into a training matrix A with size (120 by 10001).
2. The covariance of matrix A was computed giving a covariance matrix C (10001 by 10001).

3. The eigenvectors and eigenvalues were then obtained from the covariance matrix C .
4. The eigenvectors were sorted according to their corresponding eigenvalues in descending order, thus the first ones having larger variance.
5. To get the first 'x' number of principal components, the PCA transformation matrix was created using the eigenvectors with the largest 'x' eigenvalues. The size of the transformation matrix was 10001 by 'x'.
6. The PCA transformation matrix was used to project the original samples into the PCA feature space resulting into feature vectors of dimensions of 'x' by 1 representing their respective sample.
7. Step 5 and 6 were repeated for 'x' equal to 2, 5, 10, 20, 30, 40, 50, 60, 70, 80, 90 and 100.

Databases were created to contain the samples of each condition in the PCA feature space. Since one of the targets of the study is to evaluate the effect of the number of principal components used on the performance of the system, 12 separate databases were created and each one contained 120 samples (24 per class). The first 2, 5, 10, 20, 30, 40, 50, 60, 70, 80, 90 and 100 principal components were considered as the inputs for the classifiers. Figure 6.1.c gives the scatterplot of the data in PCA feature space using the first 2 principal components.



6.2. Classification Results

After the database was created, experiments were performed to evaluate the two classification schemes studied in this work.

6.2.1. Classification Scheme 1

In the first scheme, an input sample was classified directly into the condition as either healthy or faulty (together with the severity).

This scheme used the database with the 120 samples (24 samples per class) as the input signals. A five-fold cross validation method was used to evaluate the performance of the SVM classifiers with different kernel functions.

Tables 2-7 show the classification accuracy of the different classifiers used for the conditions. From the results of the experiments, it was seen that the detection accuracy as well as the severity classification accuracy of the Coarse Gaussian SVM classifier was poor. Using the other kernel functions produced higher and more reasonable results. The best overall recognition rate was realized by the ‘Cubic SVM/2 principal components’ (95%), followed by ‘Linear SVM/2 principal components’ and

‘Quadratic SVM/2 principal components’ at second (92.5%). Although the Medium Gaussian SVM classifier produced reasonable accuracy with 2 principal components, the accuracy drops drastically with the increase in the number of features used. Despite some of the classifiers achieving high accuracy in classifying the fault into their appropriate severity category, the false positive rate (i.e. healthy motors being categorized as faulty) and the false negative rate (i.e. faulty motors categorized as healthy) are still high in some of them. The three best performing systems built from Scheme 1 had the false positive and false negative rates as shown in table 1. The confusion matrices of the methods are given in the figures 6.2.1(a-d). 1, 2, 3, 4 and 5 represent ‘Healthy’, 1 broken bar, 2 broken bars, 3 broken bars and half-broken bar respectively.

SVM Kernel/No. of Features Used	Average Accuracy (%)	False Positive Rate (%)	False Negative Rate (%)
Cubic / 2	95	8.3	0
Linear / 2	92.5	8.3	2.08
Quadratic / 2	92.5	4.2	3.125
Medium Gaussian / 2	92.5	4.2	4.167

Table 1 : Overall Accuracies, False Positive and False Negative Rates of the Best Performing Methods

True class	1	22 91.7%	1 4.2%	0 0.0%	1 4.2%	0 0.0%
	2	0 0.0%	23 95.8%	1 4.2%	0 0.0%	0 0.0%
	3	0 0.0%	0 0.0%	24 100%	0 0.0%	0 0.0%
	4	0 0.0%	0 0.0%	1 4.2%	22 91.7%	1 4.2%
	5	0 0.0%	0 0.0%	0 0.0%	1 4.2%	23 95.8%
		1	2	3	4	5
		Predicted class				

Figure 6.2.1.a: Confusion Matrix for Cubic SVM with 2 Principal Components as inputs

True class	1	22 91.7%	0 0.0%	1 4.2%	1 4.2%	0 0.0%
	2	2 8.3%	22 91.7%	0 0.0%	0 0.0%	0 0.0%
	3	0 0.0%	1 4.2%	23 95.8%	0 0.0%	0 0.0%
	4	0 0.0%	0 0.0%	2 8.3%	22 91.7%	0 0.0%
	5	0 0.0%	0 0.0%	0 0.0%	2 8.3%	22 91.7%
		1	2	3	4	5
		Predicted class				

Figure 6.2.1.b: Confusion Matrix for Linear SVM with first 2 principal components as inputs

True class	1	23 95.8%	0 0.0%	0 0.0%	1 4.2%	0 0.0%
	2	2 8.3%	20 83.3%	2 8.3%	0 0.0%	0 0.0%
	3	0 0.0%	0 0.0%	24 100%	0 0.0%	0 0.0%
	4	0 0.0%	0 0.0%	1 4.2%	22 91.7%	1 4.2%
	5	1 4.2%	0 0.0%	0 0.0%	1 4.2%	22 91.7%
		1	2	3	4	5
		Predicted class				

Figure 6.2.1.c: Confusion Matrix for Quadratic SVM with first 2 principal components as inputs

True class	1	23 95.8%	0 0.0%	0 0.0%	1 4.2%	0 0.0%
	2	4 16.7%	20 83.3%	0 0.0%	0 0.0%	0 0.0%
	3	0 0.0%	1 4.2%	23 95.8%	0 0.0%	0 0.0%
	4	0 0.0%	0 0.0%	1 4.2%	23 95.8%	0 0.0%
	5	0 0.0%	0 0.0%	0 0.0%	2 8.3%	22 91.7%
		1	2	3	4	5
		Predicted class				

Figure 6.2.1.d: Confusion Matrix of Medium Gaussian SVM with 2 Principal Components

Linear SVM						
No. of Principle Components	Healthy	Half BRB	1 BRB	2 BRB	3 BRB	Overall
2	91.7	91.7	91.7	95.8	91.7	92.5
5	83.3	91.7	87.5	91.7	91.7	89.2
10	91.7	91.7	91.7	91.7	87.5	90.8
20	83.3	87.5	91.7	91.7	87.5	88.34
30	83.3	95.8	95.8	91.7	83.3	89.98
40	83.3	95.8	100	95.8	83.3	91.64
50	83.3	95.8	95.8	95.8	87.5	91.64
60	87.5	95.8	95.8	87.5	87.5	90.82
70	83.3	95.8	95.8	87.5	79.2	88.32
80	83.3	95.8	95.8	91.7	87.5	90.82
90	83.3	91.7	91.7	87.5	87.5	88.34
100	83.3	83.3	100	91.7	87.5	89.16

Table 2 : Recognition Rate for Scheme 1 using Linear SVM

Quadratic SVM						
No. of Principle Components	Healthy	Half BRB	1 BRB	2 BRB	3 BRB	Overall
2	95.8	91.7	83.3	100	91.7	92.5
5	75	87.5	87.5	95.8	91.7	87.5

10	79.2	87.5	91.7	100	95.8	90.8
20	79.2	87.5	91.7	91.7	91.7	88.36
30	83.3	87.5	91.7	95.8	87.5	89.16
40	83.3	87.5	91.7	91.7	91.7	89.18
50	70.8	87.5	91.7	100	91.7	88.34
60	79.2	87.5	91.7	100	91.7	90.02
70	79.2	87.5	95.8	95.8	91.7	90
80	79.2	87.5	95.8	95.8	91.7	90
90	75	87.5	87.5	95.8	91.7	87.5
100	70.8	87.5	95.8	95.8	91.7	88.32

Table 3 : Recognition Rate for Scheme 1 using Quadratic SVM

Cubic SVM						
No. of Principle Components	Healthy	Half BRB	1 BRB	2 BRB	3 BRB	Overall
2	91.7	95.8	95.8	100	91.7	95
5	75	95.8	87.5	95.8	91.7	89.2
10	79.2	91.7	91.7	100	95.8	91.7
20	66.7	95.8	87.5	91.7	91.7	86.68
30	79.2	95.8	91.7	87.5	83.3	87.5
40	83.3	95.8	91.7	91.7	87.5	90
50	83.3	95.8	95.8	91.7	87.5	90.82
60	79.2	95.8	95.8	95.8	83.3	89.98
70	83.3	100	95.8	87.5	87.5	90.82
80	79.2	95.8	95.8	91.7	87.5	90
90	70.8	95.8	91.7	91.7	87.5	87.5
100	66.7	95.8	100	87.5	83.3	86.66

Table 4 : Recognition Rate for Scheme 1 using Cubic SVM

Fine Gaussian SVM						
No. of Principle Components	Healthy	Half BRB	1 BRB	2 BRB	3 BRB	Overall
2	87.5	95.8	83.3	91.7	87.5	89.2
5	87.5	100	87.5	95.8	91.5	92.5
10	87.5	100	79.2	95.8	95.8	91.7
20	83.3	100	70.8	87.5	83.3	84.98
30	83.3	100	75	87.5	83.3	85.82
40	83.3	100	79.2	87.5	87.5	87.5
50	87.5	100	70.8	87.5	87.5	86.66
60	83.3	100	62.5	87.5	87.5	84.16
70	83.3	100	70.8	87.5	87.5	85.82
80	83.3	95.8	66.7	83.3	79.2	81.66
90	83.3	95.8	70.8	83.3	87.5	84.14
100	70.8	95.8	75	87.5	87.5	83.32

Table 5 : Recognition Rate for Scheme 1 using Fine Gaussian SVM

Medium Gaussian SVM						
No. of Principle Components	Healthy	Half	1	2	3	Overall

		BRB	BRB	BRB	BRB	
2	95.8	91.7	83.3	95.8	95.8	92.5
5	87.5	91.7	75	91.7	91.7	87.5
10	66.7	95.8	79.2	91.7	95.8	85.84
20	25	87.5	83.3	91.7	87.5	75
30	37.5	95.8	87.5	91.7	91.7	80.84
40	25	91.7	87.5	95.8	91.7	78.34
50	33.3	87.5	95.8	95.8	87.5	79.98
60	16.7	95.8	91.7	91.7	91.7	77.52
70	29.2	95.8	91.7	87.5	87.5	78.34
80	29.2	95.8	87.5	91.7	91.7	79.18
90	29.2	95.8	83.3	91.7	91.7	78.34
100	16.7	95.8	100	95.8	95.8	80.82

Table 6 : Recognition Rate for Scheme 1 using Medium Gaussian SVM

Coarse Gaussian SVM						
No. of Principle Components	Healthy	Half BRB	1 BRB	2 BRB	3 BRB	Overall
2	16.7	45.8	87.5	87.5	70.8	61.7
5	16.7	45.8	79.2	83.3	75	60
10	16.7	41.7	100	83.3	79.2	64.18
20	8.3	41.7	79.2	83.3	75	57.5
30	8.3	41.7	100	87.5	70.8	61.66
40	16.7	37.5	79.2	83.3	75	58.34
50	16.7	45.8	95.8	83.3	75	63.32
60	12.5	45.8	91.7	83.3	75	61.66
70	0	37.5	100	83.3	79.2	60
80	8.3	37.5	95.8	83.3	70.8	59.14
90	12.5	45.8	91.7	87.5	75	62.5
100	20.8	45.8	79.2	83.3	75	60.82

Table 7 : Recognition Rate for Scheme 1 using Coarse Gaussian SVM

6.2.2. Classification Scheme 2

In the second scheme proposed, the diagnosis of the motor was given in two steps. Firstly, the motor was diagnosed as either healthy or faulty and if faulty, the severity of the fault was given in the second part. These two steps were evaluated separately.

To test the performance of the first step, the data were divided into 4 datasets. Each dataset had 24 samples of the 'healthy' class and 24 samples of the faulty class (6 samples from each severity level). Tables 8-13 give the average accuracy of the system

in fault detection using the different classifiers studied. Tables 14-19 give the accuracy of the system in classification of the faults according to their severity. For this step, the SVM with the Coarse, Medium and Fine Gaussian kernels produced the worst performance in that order starting from the worst. Quadratic SVM produced better results but still unacceptable for industrial applications. Linear (with 2 principal components) and cubic (with 5 and 10 principal components) SVM methods produced the best results. Of the two, Linear SVM had lower False Positive and False Negative rates. For step 2 (categorizing according to severity), all the SVM classifiers produced reasonable accuracy except for the coarse Gaussian SVM.

Linear SVM			
No. of Principle Components	Healthy	Faulty	Overall
2	95.80	95.80	95.80
5	95.80	90.65	93.23
10	94.78	89.60	92.19
20	93.73	81.25	87.49
30	93.75	80.23	86.99
40	93.75	83.35	88.55
50	92.70	82.28	87.49
60	92.73	77.10	84.91
70	92.73	84.38	88.55
80	93.75	84.38	89.06
90	89.58	86.45	88.01
100	91.68	83.35	87.51

Table 8 : Average Recognition rate of Linear SVM (Scheme 2 Step 1)

Quadratic SVM			
No. of Principle Components	Healthy	Faulty	Overall
2	91.68	89.60	90.64
5	88.55	87.53	88.04
10	84.40	83.35	83.88
20	84.40	81.25	82.83
30	87.50	80.23	83.86
40	88.55	81.25	84.90
50	90.65	81.25	85.95
60	88.55	82.28	85.41
70	83.35	84.38	83.86
80	86.45	78.13	82.29

90	82.30	82.30	82.30
100	84.38	78.15	81.26

Table 9 : Average Recognition rate of Quadratic SVM (Scheme 2 Step 1)

Cubic SVM			
No. of Principle Components	Healthy	Faulty	Overall
2	90.63	91.65	91.14
5	91.65	94.78	93.21
10	94.78	92.70	93.74
20	85.43	89.58	87.50
30	85.40	93.75	89.58
40	90.63	92.73	91.68
50	89.58	92.70	91.14
60	86.48	90.63	88.55
70	84.40	91.68	88.04
80	85.43	87.50	86.46
90	79.18	91.68	85.43
100	79.15	87.48	83.31

Table 10 : Average Recognition rate of Cubic SVM (Scheme 2 Step 1)

Fine Gaussian SVM			
No. of Principle Components	Healthy	Faulty	Overall
2	86.45	79.18	82.81
5	80.20	77.10	78.65
10	80.23	72.90	76.56
20	84.38	76.05	80.21
30	83.33	72.93	78.13
40	85.40	73.95	79.68
50	80.20	75.00	77.60
60	81.23	71.85	76.54
70	82.30	75.00	78.65
80	80.23	76.05	78.14
90	82.30	73.95	78.13
100	81.25	76.03	78.64

Table 11 : Average Recognition rate of Fine Gaussian SVM (Scheme 2 Step 1)

Medium Gaussian SVM			
No. of Principle Components	Healthy	Faulty	Overall Performance
2	95.80	56.25	76.03
5	91.70	57.30	74.50
10	89.60	55.20	72.40
20	90.63	55.23	72.93
30	91.68	53.10	72.39
40	91.70	55.23	73.46

50	92.73	54.18	73.45
60	90.65	53.10	71.88
70	90.63	55.20	72.91
80	90.65	53.10	71.88
90	91.68	51.03	71.35
100	89.60	54.15	71.88

Table 12 : Average Recognition rate of Medium Gaussian SVM (Scheme 2 Step 1)

Coarse Gaussian SVM			
No. of Principle Components	Healthy	Faulty	Overall Performance
2	96.85	26.03	61.44
5	96.85	28.10	62.48
10	96.85	25.00	60.93
20	97.90	26.03	61.96
30	96.85	25.00	60.93
40	96.85	22.93	59.89
50	96.85	25.00	60.93
60	95.80	23.95	59.88
70	97.90	24.98	61.44
80	96.85	24.98	60.91
90	96.85	23.95	60.40
100	95.80	27.08	61.44

Table 13 : Average Recognition rate of Coarse Gaussian SVM (Scheme 2 Step 1)

Linear SVM					
No. of Principle Components	Half BRB	1 BRB	2 BRB	3 BRB	Overall
2	91.7	95.8	100	91.7	94.80
5	95.8	95.8	95.8	91.7	94.78
10	95.8	95.8	100	91.7	95.83
20	95.8	95.8	95.8	91.7	94.78
30	95.8	95.8	100	91.7	95.83
40	95.8	95.8	100	95.8	96.85
50	95.8	95.8	95.8	91.7	94.78
60	95.8	95.8	100	95.8	96.85
70	95.8	100	95.8	87.5	94.78
80	95.8	100	95.8	87.5	94.78
90	95.8	91.7	95.8	87.5	92.70
100	95.8	100	95.8	87.5	94.78

Table 14 : Severity Classification Accuracy of Linear SVM (Scheme 2 Step 2)

Quadratic SVM					
No. of Principle Components	Half BRB	1 BRB	2 BRB	3 BRB	Overall
2	95.8	91.7	91.7	95.8	93.75
5	87.5	95.8	100	95.8	94.78
10	87.5	95.8	100	95.8	94.78
20	87.5	95.8	95.8	91.7	92.70
30	87.5	91.7	91.7	95.8	91.68

40	87.5	95.8	91.7	95.8	92.70
50	91.7	95.8	87.5	91.7	91.68
60	87.5	95.8	95.8	87.5	91.65
70	87.5	95.8	87.5	91.7	90.63
80	87.5	95.8	91.7	95.8	92.70
90	87.5	91.7	91.7	91.7	90.65
100	87.5	100	95.8	91.7	93.75

Table 15 : Severity Classification Accuracy of Quadratic SVM (Scheme 2 Step 2)

Cubic SVM					
No. of Principle Components	Half BRB	1 BRB	2 BRB	3 BRB	Overall
2	100	91.7	95.8	95.8	95.83
5	100	95.8	100	95.8	97.90
10	91.7	95.8	95.8	95.8	94.78
20	95.8	95.8	95.8	91.7	94.78
30	95.8	95.8	87.5	91.7	92.70
40	95.8	95.8	91.7	91.7	93.75
50	95.8	95.8	87.5	83.3	90.60
60	95.8	95.8	95.8	83.3	92.68
70	95.8	91.7	91.7	87.5	91.68
80	95.8	100	91.7	91.7	94.80
90	95.8	91.7	91.7	87.5	91.68
100	95.8	95.8	95.8	83.3	92.68

Table 16 : Severity Classification Accuracy of Cubic SVM (Scheme 2 Step 2)

Fine Gaussian SVM					
No. of Principle Components	Half BRB	1 BRB	2 BRB	3 BRB	Overall
2	100	95.8	91.7	87.5	93.75
5	100	95.8	95.8	95.8	96.85
10	95.8	95.8	95.8	91.7	94.78
20	100	95.8	87.5	91.7	93.75
30	95.8	95.8	87.5	91.7	92.70
40	100	91.7	87.5	87.5	91.68
50	95.8	95.8	87.5	83.3	90.60
60	100	95.8	87.5	87.5	92.70
70	100	91.7	83.3	83.3	89.58
80	95.8	95.8	91.7	83.3	91.65
90	95.8	91.7	87.5	83.3	89.58
100	95.8	100	95.8	83.3	93.73

Table 17 : Severity Classification Accuracy of Fine Gaussian SVM (Scheme 2 Step 2)

Medium Gaussian SVM					
No. of Principle Components	Half BRB	1 BRB	2 BRB	3 BRB	Overall
2	100	95.8	91.7	87.5	93.75
5	91.7	95.8	95.8	91.7	93.75
10	91.7	95.8	100	91.7	94.80
20	95.8	95.8	95.8	91.7	94.78
30	95.8	95.8	87.5	91.7	92.70

40	91.7	95.8	100	91.7	94.80
50	95.8	95.8	95.8	87.5	93.73
60	91.7	95.8	100	91.7	94.80
70	91.7	95.8	95.8	91.7	93.75
80	95.8	100	95.8	91.7	95.83
90	87.5	95.8	95.8	91.7	92.70
100	95.8	100	95.8	95.8	96.85

Table 18 : Severity Classification Accuracy of Medium Gaussian SVM (Scheme 2 Step 2)

Coarse Gaussian SVM					
No. of Principle Components	Half BRB	1 BRB	2 BRB	3 BRB	Overall
2	45.8	100	95.8	79.2	80.20
5	45.8	95.8	95.8	83.3	80.18
10	41.7	95.8	95.8	83.3	79.15
20	50	95.8	95.8	79.2	80.20
30	41.7	100	95.8	83.3	80.20
40	50	95.8	100	83.3	82.28
50	41.7	95.8	100	79.2	79.18
60	37.5	95.8	100	83.3	79.15
70	45.8	100	95.8	83.3	81.23
80	41.7	100	91.7	83.3	79.18
90	45.8	100	100	83.3	82.28
100	45.8	100	95.8	83.3	81.23

Table 19 : Severity Classification Accuracy of Coarse Gaussian SVM (Scheme 2 Step 2)

7. DISCUSSION AND CONCLUSION

7.1 Discussion

In this study 2 classification schemes (namely Scheme 1 and Scheme 2) for the detection of BRBs and classification according to severity were developed from experimental work.

Scheme 1 gives diagnosis in one step and Scheme 2 in 2 steps. For the algorithm to be suitable in an industrial setting it should be able to distinguish accurately between healthy and faulty motors. Therefore it is important to analyse the False Positive and False Negative Rates to avoid false alarms as well as to avoid faults going undetected.

When comparing the methods created from the 2 schemes, the cubic SVM method with 2 principal components as inputs created from scheme 1 proved to produce the best fault detection results with zero False Negative rate recorded from the experiments; that is, no faulty motor was undetected. False Positive rate was recorded at 8.3%, thus an increased rate of false alarms. In comparison, the best performing system developed by scheme 2 for fault detection (Linear SVM with 2 principal components as input), had 4.2% false positive rate and 4.2% false negative rates. Although this shows an improvement in preventing false alarms, there is an increased risk of faults going undetected.

For the purpose of fault classification, the methods created using scheme 2 produced better severity classification results in general. The best overall performance for this purpose was recorded at 97.9% when using cubic SVM with 5 principal components as inputs. The rest of the SVM classifiers that use different kernel functions (except for Coarse Gaussian SVM) also produced reasonable classification rates (refer to the tables in the classification results section).

7.2 Conclusion

In this study a series of experiments were performed to simulate broken rotor bar faults in induction motors; and the aim was to use the experimental data to develop a machine learning system that would detect the problem as well as provide its severity. The motor current was used as the monitoring signal and feature extraction was performed using PCA transformation on the current signals in frequency domain.

Two schemes were developed for classification, Scheme 1 that performs the classification in one go and Scheme 2 that first detects if there's a fault then gives the severity. Both schemes produced some fault diagnosis systems that gave reasonable results. Using Scheme 1, cubic SVM with 2 principal components as inputs was able to produce zero false negative rate. However the false positive rate was still high at 8.3%. For severity classification, the methods created using scheme 2 showed better accuracy. Also, there was improvement in the false positive rate in fault detection's best performer (Linear SVM with 2 principal components as input); recorded at 4.2%. However the false negative rate was recorded at 4.2, hence a risk for faults being undetected.

Furthermore no significant improvement was seen from using more principal components as input. In fact lesser number of features proved more effective in detection and classification and more efficient as the diagnosis is given faster.

REFERENCES

- Abbaszadeh, K., Milimonfared, J., Haji, M. ve Toliyat, H., 2001, Broken bar detection in induction motor via wavelet transformation, *IECON'01. 27th Annual Conference of the IEEE Industrial Electronics Society (Cat. No. 37243)*, 95-99.
- Afifi, A., 2014, Laguerre kernels-based SVM for image classification, *International Journal of Advanced Computer Science and Applications*, 5 (1).
- Ali, M. Z., Shabbir, M. N. S. K., Liang, X., Zhang, Y. ve Hu, T., 2018, Experimental Investigation of Machine Learning Based Fault Diagnosis for Induction Motors, *2018 IEEE Industry Applications Society Annual Meeting (IAS)*, 1-14.
- Ali, M. Z., Shabbir, M. N. S. K., Liang, X., Zhang, Y. ve Hu, T., 2019, Machine Learning-Based Fault Diagnosis for Single-and Multi-Faults in Induction Motors Using Measured Stator Currents and Vibration Signals, *IEEE Transactions on Industry Applications*, 55 (3), 2378-2391.
- Arabacı, H. ve Bilgin, O., 2010, Automatic detection and classification of rotor cage faults in squirrel cage induction motor, *Neural Computing and Applications*, 19 (5), 713-723.
- Arkan, M., Kostic-Perovic, D. ve Unsworth, P. J., 2005, Modelling and simulation of induction motors with inter-turn faults for diagnostics, *Electric Power Systems Research*, 75 (1), 57-66.
- Ayhan, B., Chow, M. Y. ve Song, M. H., 2006, Multiple discriminant analysis and neural-network-based monolith and partition fault-detection schemes for broken rotor bar in induction motors, *IEEE Transactions on Industrial Electronics*, 53 (4), 1298-1308.
- Bacha, K., Salem, S. B. ve Chaari, A., 2012, An improved combination of Hilbert and Park transforms for fault detection and identification in three-phase induction motors, *International Journal of Electrical Power & Energy Systems*, 43 (1), 1006-1016.
- Barnouti, N. H., Al-Dabbagh, S. S. M., Matti, W. E. ve Naser, M. A. S., 2016, Face Detection and Recognition Using Viola-Jones with PCA-LDA and Square Euclidean Distance, *International Journal of Advanced Computer Science and Applications (IJACSA)*, 7 (5), 371-377.
- Benbouzid, M. E. H., Vieira, M. ve Theys, C., 1999, Induction motors' faults detection and localization using stator current advanced signal processing techniques, *IEEE Transactions on power electronics*, 14 (1), 14-22.
- Benbouzid, M. E. H., 2000, A review of induction motors signature analysis as a medium for faults detection, *IEEE Transactions on Industrial Electronics*, 47 (5), 984-993.
- Benbouzid, M. E. H. ve Kliman, G. B., 2003, What stator current processing-based technique to use for induction motor rotor faults diagnosis?, *IEEE Transactions on Energy Conversion*, 18 (2), 238-244.
- Bossio, J. M., De Angelo, C. H. ve Bossio, G. R., 2013, Self-organizing map approach for classification of mechanical and rotor faults on induction motors, *Neural Computing and Applications*, 23 (1), 41-51.
- Cameron, J., Thomson, W. ve Dow, A., 1986, Vibration and current monitoring for detecting airgap eccentricity in large induction motors, *IEE Proceedings B (Electric Power Applications)*, 155-163.

- Cardoso, A. J. M., Cruz, S. M. A. ve Fonseca, D. S. B., 1999, Inter-turn stator winding fault diagnosis in three-phase induction motors, by Park's vector approach, *IEEE Transactions on Energy Conversion*, 14 (3), 595-598.
- Chow, T. W. S. ve Fei, G., 1995, Three phase induction machines asymmetrical faults identification using bispectrum, *IEEE Transactions on Energy Conversion*, 10 (4), 688-693.
- De Angelo, C. H., Bossio, G. R. ve Garcia, G. O., 2010, Discriminating broken rotor bar from oscillating load effects using the instantaneous active and reactive powers, *IET electric power applications*, 4 (4), 281-290.
- Ebrahimi, B. M., Roshtkhari, M. J., Faiz, J. ve Khatami, S. V., 2013, Advanced eccentricity fault recognition in permanent magnet synchronous motors using stator current signature analysis, *IEEE Transactions on Industrial Electronics*, 61 (4), 2041-2052.
- Edomwandekhoe, K. I., 2018, Modeling and fault diagnosis of broken rotor bar faults in induction motors, *Memorial University of Newfoundland*.
- Ertunc, H. M., Ocaik, H. ve Aliustaoglu, C., 2013, ANN-and ANFIS-based multi-staged decision algorithm for the detection and diagnosis of bearing faults, *Neural Computing and Applications*, 22 (1), 435-446.
- Faiz, J., Ebrahimi, B. M. ve Toliyat, H. A., 2007, Signature analysis of electrical and mechanical signals for diagnosis of broken rotor bars in an induction motor, *Electromagnetics*, 27 (8), 507-526.
- Gangsar, P. ve Tiwari, R., 2017, Comparative investigation of vibration and current monitoring for prediction of mechanical and electrical faults in induction motor based on multiclass-support vector machine algorithms, *Mechanical Systems and Signal Processing*, 94, 464-481.
- Ghate, V. N. ve Dudul, S. V., 2010, Design of optimal MLP and RBF neural network classifier for fault diagnosis of three phase induction motor, *International Journal of Advanced Mechatronic Systems*, 2 (3), 204-216.
- Haji, M. ve Toliyat, H. A., 2001, Pattern recognition-a technique for induction machines rotor fault detection" eccentricity and broken bar fault", *Conference Record of the 2001 IEEE Industry Applications Conference. 36th IAS Annual Meeting (Cat. No. 01CH37248)*, 1572-1578.
- Hajiaghajani, M., Toliyat, H. A. ve Panahi, I. M. S., 2004, Advanced fault diagnosis of a DC motor, *IEEE Transactions on Energy Conversion*, 19 (1), 60-65.
- Heller, B. ve Hamata, V., 1977, Harmonic field effects in induction machines, Elsevier Science & Technology, p.
- Ikeda, M. ve Hiyama, T., 2007, Simulation studies of the transients of squirrel-cage induction motors, *IEEE Transactions on Energy Conversion*, 22 (2), 233-239.
- Ilonen, J., Kamarainen, J. K., Lindh, T., Ahola, J., Kalviainen, H. ve Partanen, J., 2005, Diagnosis tool for motor condition monitoring, *IEEE Transactions on Industry Applications*, 41 (4), 963-971.
- Kliman, G. ve Stein, J., 1990, Induction motor fault detection via passive current monitoring-A brief survey, *Proc. 44th Meeting of the Mechanical Failures Prevention Group*, 49-65.
- Kliman, G. B. ve Stein, J., 1992, Methods of motor current signature analysis, *Electric Machines and power systems*, 20 (5), 463-474.
- Konar, P. ve Chattopadhyay, P., 2011, Bearing fault detection of induction motor using wavelet and Support Vector Machines (SVMs), *Applied Soft Computing*, 11 (6), 4203-4211.

- Legowski, S. F., Ula, A. H. M. S. ve Trzynadlowski, A. M., 1996, Instantaneous power as a medium for the signature analysis of induction motors, *IEEE Transactions on Industry Applications*, 32 (4), 904-909.
- Li, B., Chow, M. Y., Tipsuwan, Y. ve Hung, J. C., 2000, Neural-network-based motor rolling bearing fault diagnosis, *IEEE Transactions on Industrial Electronics*, 47 (5), 1060-1069.
- Liang, B., Payne, B. S., Ball, A. D. ve Iwnicki, S. D., 2002, Simulation and fault detection of three-phase induction motors, *Mathematics and computers in simulation*, 61 (1), 1-15.
- Liu, R., Yang, B., Zio, E. ve Chen, X., 2018, Artificial intelligence for fault diagnosis of rotating machinery: A review, *Mechanical Systems and Signal Processing*, 108, 33-47.
- Liu, Y. ve Bazzi, A. M., 2017, A review and comparison of fault detection and diagnosis methods for squirrel-cage induction motors: State of the art, *ISA transactions*, 70, 400-409.
- MA Cruz, A. J. M. C. S., 2000, Rotor cage fault diagnosis in three-phase induction motors by extended Park's vector approach, *Electric Machines & Power Systems*, 28 (4), 289-299.
- Maier, R., 1992, Protection of squirrel-cage induction motor utilizing instantaneous power and phase information, *IEEE Transactions on Industry Applications*, 28 (2), 376-380.
- Martins, J. F., Pires, V. F. ve Pires, A. J., 2007, Unsupervised neural-network-based algorithm for an on-line diagnosis of three-phase induction motor stator fault, *IEEE Transactions on Industrial Electronics*, 54 (1), 259-264.
- Matić, D., Kulić, F., Pineda-Sánchez, M. ve Kamenko, I., 2012, Support vector machine classifier for diagnosis in electrical machines: Application to broken bar, *Expert Systems with Applications*, 39 (10), 8681-8689.
- Mirafzal, B. ve Demerdash, N. A. O., 2005, Effects of load magnitude on diagnosing broken bar faults in induction motors using the pendulous oscillation of the rotor magnetic field orientation, *IEEE Transactions on Industry Applications*, 41 (3), 771-783.
- Nandi, S., Toliyat, H. A. ve Li, X., 2005, Condition monitoring and fault diagnosis of electrical motors—A review, *IEEE Transactions on Energy Conversion*, 20 (4), 719-729.
- Ojaghi, M., Sabouri, M. ve Faiz, J., 2014, Diagnosis methods for stator winding faults in three-phase squirrel-cage induction motors, *International transactions on electrical energy systems*, 24 (6), 891-912.
- Ondel, O., Boutleux, E. ve Clerc, G., 2006, A method to detect broken bars in induction machine using pattern recognition techniques, *IEEE Transactions on Industry Applications*, 42 (4), 916-923.
- Ozgonenel, O. ve Yalcin, T., 2010, Principal component analysis (PCA) based neural network for motor protection, *10th IET International Conference on Developments in Power System Protection (DPSP 2010). Managing the Change*, 1-5.
- Palácios, R. H. C., da Silva, I. N., Goedtel, A. ve Godoy, W. F., 2015, A comprehensive evaluation of intelligent classifiers for fault identification in three-phase induction motors, *Electric Power Systems Research*, 127, 249-258.
- Pearson, K., 1901, LIII. On lines and planes of closest fit to systems of points in space, *The London, Edinburgh, and Dublin Philosophical Magazine and Journal of Science*, 2 (11), 559-572.

- Peng, H.-W. ve Chiang, P.-J., 2011, Control of mechatronics systems: Ball bearing fault diagnosis using machine learning techniques, *2011 8th Asian Control Conference (ASCC)*, 175-180.
- Pezzani, C. M., Fontana, J. M., Donolo, P. D., De Angelo, C. H., Bossio, G. R. ve Silva, L. I., 2018, SVM-Based System for Broken Rotor Bar Detection in Induction Motors, *2018 IEEE ANDESCON*, 1-6.
- Puche-Panadero, R., Pineda-Sanchez, M., Riera-Guasp, M., Roger-Folch, J., Hurtado-Perez, E. ve Perez-Cruz, J., 2009a, Improved resolution of the MCSA method via Hilbert transform, enabling the diagnosis of rotor asymmetries at very low slip, *IEEE Transactions on Energy Conversion*, 24 (1), 52-59.
- Puche-Panadero, R., Pons-Llinares, J., Climente-Alarcon, V. ve Pineda-Sanchez, M., 2009b, Review diagnosis methods of induction electrical machines based on steady state current, *XI Portuguese-Spanish conference in electrical engineering (XICLEEE)*.
- Saddam, B., Ahmed, B. S., Aissa, A. ve Ali, T., 2018, Squirrel Cage Induction Motor under Stator and Rotor Bars Faults Modeling and Diagnosis, *2018 International Conference on Communications and Electrical Engineering (ICCEE)*, 1-6.
- Seera, M., Lim, C. P., Nahavandi, S. ve Loo, C. K., 2014, Condition monitoring of induction motors: A review and an application of an ensemble of hybrid intelligent models, *Expert Systems with Applications*, 41 (10), 4891-4903.
- Siau, J. M. B., Graff, A. L., Soong, W. L. ve Ertugrul, N., 2004, Broken bar detection in induction motors using current and flux spectral analysis, *Australian Journal of Electrical and Electronics Engineering*, 1 (3), 171-178.
- Su, H. ve Chong, K. T., 2007, Induction machine condition monitoring using neural network modeling, *IEEE Transactions on Industrial Electronics*, 54 (1), 241-249.
- Taher, S. A. ve Malekpour, M., 2011, A novel technique for rotor bar failure detection in single-cage induction motor using FEM and MATLAB/SIMULINK, *Mathematical Problems in Engineering*, 2011.
- Tan, W. W. ve Huo, H., 2005, A generic neurofuzzy model-based approach for detecting faults in induction motors, *IEEE Transactions on Industrial Electronics*, 52 (5), 1420-1427.
- Thomson, W. T. ve Fenger, M., 2001, Current signature analysis to detect induction motor faults, *IEEE Industry Applications Magazine*, 7 (4), 26-34.
- Trzynadlowski, A. M., Ghassemzadeh, M. ve Legowski, S. F., 1999, Diagnostics of mechanical abnormalities in induction motors using instantaneous electric power, *IEEE Transactions on Energy Conversion*, 14 (4), 1417-1423.
- Vapnik, V., Levin, E. ve Cun, Y. L., 1994, Measuring the VC-dimension of a learning machine, *Neural computation*, 6 (5), 851-876.
- Vas, P., 1993, Parameter estimation, condition monitoring, and diagnosis of electrical machines, Oxford University Press, p.
- Wang, J., Liu, S., Gao, R. X. ve Yan, R., 2012, Current envelope analysis for defect identification and diagnosis in induction motors, *Journal of Manufacturing Systems*, 31 (4), 380-387.
- Zhongming, Y. ve Bin, W., 2000, A review on induction motor online fault diagnosis, *Proceedings IPEMC 2000. Third International Power Electronics and Motion Control Conference (IEEE Cat. No. 00EX435)*, 1353-1358.

RESUME

PERSONAL INFORMATION

Name Surname : Mohamed Ali MOHAMED
Nationality : Kenyan
Birth Place and Date : Mombasa , Kenya / 1992
Telephone Number : 0553 216 82 76
Fax : -
e-mail : mohamedsaary04@gmail.com

EDUCATION

Degree	Name, Province, City	Completed
High School	: Sheikh Khalifa Bin Zayed Al-Nahyan Secondary and Technical School (Mombasa, Kenya)	2010
University	: Mevlana Üniversitesi (Konya, Turkey)	2015
Masters	: Selçuk Üniversitesi (Konya, Turkey)	2019

PUBLICATIONS

Error Analysis of a Practical Technique for Transforming Welding Seam Features to the Robot Base Coordinate Frame

RESEARCH INTERESTS

Pattern Recognition
 Machine Learning
 Image/Signal Processing

LANGUAGES

English
 Swahili
 Arabic
 Turkish